

Mareks Parfjonovs

DEVELOPMENT OF A HYBRID BROADBAND AMPLIFIER FOR FOTS SOLUTIONS

Summary of the Doctoral Thesis



RIGA TECHNICAL UNIVERSITY

Faculty of Computer Science, Information Technology and Energy
Institute of Photonics, Electronics and Electronic Communications

Mareks Parfjonovs

Doctoral Student of the Study Programme “Telecommunications”

**DEVELOPMENT OF A HYBRID BROADBAND
AMPLIFIER FOR FOTS SOLUTIONS**

Summary of the Doctoral Thesis

Scientific supervisor

Professor Dr. sc. ing.

VJAČESLAVS BOBROVS

RTU Press

Riga 2024

Parfjonovs, M. Development of a Hybrid Broadband Amplifier for FOTS Solutions. Summary of the Doctoral Thesis. Riga: RTU Press, 2024. 42 p.

Published in accordance with the decision of the Promotion Council “RTU P-08” of 8 December 2023, Minutes No. 27

This work has been supported by the European Social Fund within Project No. 8.2.2.0/20/I/008, “Strengthening of PhD students and academic personnel of Riga Technical University and BA School of Business and Finance in the strategic fields of specialization” of the Specific Objective 8.2.2 “To Strengthen Academic Staff of Higher Education Institutions in Strategic Specialization Areas” of the Operational Programme “Growth and Employment”.

**NATIONAL
DEVELOPMENT
PLAN 2020**



EUROPEAN UNION
European Social
Fund

I N V E S T I N G I N Y O U R F U T U R E

<https://doi.org/10.7250/9789934370335>

ISBN 978-9934-37-033-5 (pdf)

DOCTORAL THESIS PROPOSED TO RIGA TECHNICAL UNIVERSITY FOR THE PROMOTION TO THE SCIENTIFIC DEGREE OF DOCTOR OF SCIENCE

To be granted the scientific degree of Doctor of Engineering Science (Ph. D.), the present Doctoral Thesis has been submitted for defence at the open meeting of RTU Promotion Council on February 23rd, 2024, at 15:00 at the Faculty of Computer Science, Information Technology and Energy of Riga Technical University, 12 Āzenes Street, Room 201.

OFFICIAL REVIEWERS

Associate Professor Dr. sc. ing. Aleksandrs Ipatovs
Riga Technical University

Professor Dr. sc. comp. Anita Jansone
University of Liepāja, Latvia

Associate Professor Dr. phys. Jānis Alnis
University of Latvia, Latvia

DECLARATION OF ACADEMIC INTEGRITY

I hereby declare that the Doctoral Thesis submitted for review to Riga Technical University for promotion to the scientific degree of Doctor of Engineering Science (Ph. D.) is my own. I confirm that this Doctoral Thesis has not been submitted to any other university for promotion to a scientific degree.

Mareks Parfjonovs (signature)

Date:

The Doctoral Thesis has been written in Latvian. It consists of an introduction, 3 chapters, conclusions, 77 figures, 15 tables, and 51 appendices; the total number of pages is 123, not including appendices. The Bibliography contains 160 titles.

ANNOTATION

Title of the Thesis: “*Development of a Hybrid Broadband Amplifier for FOTS Solutions*”

Author of the Thesis: Mareks Parfjonovs

The Doctoral Thesis represents a comprehensive investigation into designing, developing, and implementing an innovative hybrid broadband amplifier for fiber optical transmission systems. In response to the ever-increasing demand for higher network capacity and data transmission efficiency, this research addresses the challenges associated with optical signal amplification over extended distances in modern optical communication networks.

The core objectives of this study involve the creation of a novel hybrid amplifier that leverages the strengths of different amplification technologies while mitigating their limitations. The Thesis delves into the theoretical principles and practical considerations underlying the hybrid broadband amplifier, drawing from various optical amplifier technologies. It seeks to optimize signal quality and transmission efficiency in fiber optic networks, especially in scenarios where optical attenuation and bandwidth expansion are critical factors.

Through a rigorous exploration of the design, performance evaluation, and real-world applications of the hybrid broadband amplifier, this work contributes to advancing state-of-the-art optical communication technologies. The findings and insights presented herein have the potential to significantly enhance the capabilities of optical transmission systems and play a pivotal role in meeting the escalating demands of contemporary high-capacity data networks.

Overall, this research offers a valuable contribution to the field of fiber optical transmission and holds promise for the continued evolution and improvement of broadband communication systems.

CONTENTS

CONTENTS.....	5
ABBREVIATIONS.....	6
GENERAL DESCRIPTION OF THE RESEARCH.....	8
Topicality of the Research	8
The Aims and Tasks of the Thesis and Thesis Statements to Be Defended	8
Research Methods.....	9
Scientific Novelty and Main Results	9
Volume and Structure of the Doctoral Thesis	10
Approbation of Research Results	11
INTRODUCTION.....	13
GENERAL DESCRIPTION OF THE RESEARCH.....	15
Chapter 1	15
Chapter 2	17
Chapter 3.....	20
MAIN RESULTS OF THE DOCTORAL THESIS.....	37
BIBLIOGRAPHY	41

ABBREVIATIONS

A

APD – Avalanche photodiode
ASE – Amplified Spontaneous Emission
AWG – Arrayed Waveguide Gratings

B

BER – Bit Error Rate

C

CD – Chromatic Dispersion
 CD_{SL} – Chromatic Dispersion Slope
CO – Central Office
CW – Continuous Wave laser
CWDM – Coarse Wavelength Division Multiplexing

D

DCF – Dispersion Compensating Fiber
DCM – Dispersion Compensating Module
DEMUX – Demultiplexor
DP-QPSK – Dualpolarisation Quadrature Phase-Shift Keying
DWDM – Dense Wavelength Division Multiplexing
DWDM-PON – Dense Wavelength Division Multiplexing

F

FBG – Fiber Bragg Grating
FEC – Forward Error Correction
FOPA – Fiber Optical Parametric Amplifier
FOTS – Fiber Optical Transmission System
FP-SOA – Fabry-Perot Semiconductor Optical Amplifier

G

GN – Global Gain

H

HNLF – High Non-Linearity Fiber
HDWDM – High-Density Wavelength Division Multiplexing

I

IL – Insertion Loss
ISI – Intersymbol Interference
ITU-T – International Telecommunication Union

L

LPF – Low-Pass Filter

M

MCF – Multi-Core Fiber
MZM – Mach-Zehnder Modulator
MUX – Multiplexor

N

NB-HA – Narrowband Hybrid Amplifier

NF – Noise Figure

NOE – Nonlinear Optical Effects

NRZ – Non-Return-to-Zero

NRZ-OOK – Non-Return-to-Zero On-Off Keying

NRZ-DPSK – Non-Return-to-Zero Differential Phase Shift Keying

NZDSF – Non-Zero Dispersion Shifted Fiber

O

OBPF – Optical Band-Pass Filter

ODN – Optical Distribution Network

OF – Optical Fiber

OLT – Optical Line Terminal

OLT-Tx – Optical Line Terminal Transmitter

ONT – Optical Network Terminal

ONT-Rx – Optical Network Terminal Receiver

OSA – Optical Spectrum Analyzer

OSNR – Optical Signal-Noise Ratio

P

PIN – PIN photodiode

PMD – Polarization Mode Dispersion

PON – Passive Optical Network

PRBS – Pseudo-Random-Bit-Sequence

P2P – Point-to-Point

R

ROADM – Reconfigurable Optical Add-Drop Multiplexer

RX – Receiver

RZ – Return-to-Zero

S

S-LED – Superluminescent Light-Emitting Diode

SDM – Space Division Multiplexing

SMF – Single Mode Fiber

SNR – Signal-Noise Ratio

SOA – Semiconductor Optical Amplifier

SWB-HA – Seamless and Wideband Hybrid Amplifiers

T

TDM – Time Division Multiplexing

TW-SOA – Travelling Wave Semiconductor Optical Amplifier

TX – Transmitter

V

VOA – Variable Optical Attenuator

W

WDM – Wavelength Division Multiplexing

WSS – Wavelength Selective Switch

GENERAL DESCRIPTION OF THE RESEARCH

Topicality of the Research

According to the latest CISCO forecast, global IP data traffic will almost triple in the next 5 years. The reasons are the growing number of end users and new and improved existing quality services. Thus, higher data rates are required to ensure real-time information transmission. This creates further problems for optical transmission systems, one of which is the amplification of optical signals. The optical signal amplifier is an integral part of the set of elements of modern fiber optic transmission systems (FOTS). The range of applications of optical amplifiers is wide – from low-cost, short-distance access networks to regional networks, e.g. very long-distance intercontinental underwater networks. Optical amplifiers are also very relevant in the context of signal processing techniques based on the use of nonlinear optical effects (NOE). For example, multi-wavelength light sources, wavelength converters, all-optical regenerators, etc. Such applications typically require high optical power. Studies of the optical properties of doped fiber amplifiers have been extensive for different doping and different doping in the same fiber.

The most common amplifiers in modern optical communication systems are the erbium-doped fiber amplifier (EDFA) and the Raman fiber amplifier. Long and very long-distance networks use hybrid solutions consisting of EDFA and Raman amplifiers.

The envelope pumping method has also been extensively studied for amplifier applications. The combination of both solutions (various alloys and pumping in the core/cladding) is considered an actual research direction. However, significant additional studies of the expected amplifiers are needed to improve the gain uniformity noise ratio (signal-to-noise ratio (SNR)), ensure the efficiency of the pumping source (energy efficiency), and ensure the optical signal gain efficiency of the amplifier, etc. The main idea is to study all the latest technical solutions for doped fiber amplifiers and choose the most suitable one to develop a cost-effective amplifier that is better than the existing solutions available. It also includes searching for the most suitable doped fibers, measuring fiber optical parameters, designing unique combiners, and validation and performance evaluation of prototypes. The intended scope (but not limited) in terms of applications includes wavelength division multiplexed (WDM) optical transmission systems, metro access networks and passive optical networks (PONs) to extend transmission reach.

The Aims and Tasks of the Thesis and Thesis Statements to Be Defended

The aim of the Thesis is to develop a novel hybrid wideband optical amplifier using doped optical fibers and an efficient cladding pumping technique to improve the performance of wavelength division multiplexed (WDM) communication systems.

To achieve the aim, it was necessary to perform the following key tasks:

1. Experimentally in a mathematical modelling environment, evaluate the use of EDFA and SOA amplifiers for determining the maximum transmission distance of DP-QPSK modulation WDM communication systems with data transmission rate 100 Gbit/s per λ , without exceeding the $BER \geq 1 \times 10^{-9}$ limit value of the received signal (Q-factor level higher than 16 dB).

2. Experimentally in RTU TI FOTS laboratory, evaluate the erbium (Er^{3+})/ytterbium (Yb^{3+}) -co-doped fiber amplification efficiency depending on the doped fiber span length for the development of a novel, innovative erbium-doped fiber amplifier.
3. Experimentally in a mathematical modelling environment, evaluate the effects of chromatic dispersion (CD) and nonlinear optical effects (NOE) and their compensation methods for increasing the maximum transmission distance of the WDM communication system with a data transmission rate up to 40 Gbit/s per λ , without exceeding the $BER \geq 1 \times 10^{-9}$ limit value of the received signal.
4. Develop a hybrid Raman-EDFA amplifier and evaluate its performance in a 16-channel DWDM communication system with a data transmission rate of 10 Gbit/s per channel without exceeding the received signal's $BER \geq 1 \times 10^{-9}$ limit value.

To achieve the aim, the following theses were put forward:

1. In erbium (Er^{3+})/ytterbium (Yb^{3+}) -co-doped fibers, the highest signal gain is obtained in the first 3 meters, while increasing the length of the -co-doped fiber above 5 meters ensures the preservation of the gain level and its transfer to longer light wavelengths.
2. Using the hybrid EDFA-Raman amplifier in the WDM communication system, it is possible to simultaneously ensure the amplification of optical carriers in the entire C-band (1530–1565 nm) and reduce the accumulated chromatic dispersion CD-induced intersymbol interference (ISI), ensuring the maximum line transmission distance.

Research Methods

To perform the tasks outlined in the Doctoral Thesis and to analyze the problems, mathematical calculations, numerical simulations, and experimental measurements have been used. Numerical simulations were implemented in RSoft OptSim simulation software based on the nonlinear Schrödinger equation using the split-step method, the Fourier transform, and the Monte Carlo method for estimating the bit-error-rate (BER).

The quality of the received electrical signals was evaluated using bit error rate (BER) and eye diagrams. In the implementation of experimental systems, in some cases, the quality of electrical signals received in real-time measurements was evaluated by the signal bit error ratio (BER). The scientific research experiments described in the dissertation and their results have been implemented at the Telecommunications Institute of RTU (TI), Latvia.

Scientific Novelty and Main Results

Novel achievements of the Doctoral Thesis

1. The use of EDFA and SOA amplifiers was evaluated in terms of maximum transmission distance for WDM communication systems, depending on the data transmission rate in the channel, by using several modulation formats (NRZ, RZ, DP-QPSK), without exceeding the $BER \geq 1 \times 10^{-9}$ limit value of the received signal.
2. The use of erbium (Er^{3+})/ytterbium (Yb^{3+}) -co-doped fiber was evaluated in the creation of a novel, innovative optical erbium-doped amplifier, determining the amplification efficiency depending on the co-doped fiber span length.

3. Based on the requirements of today's fiber optic high-speed communication systems, e.g. the conditions set for the data transmission rate in the channel (at least 40 Gbit/s per λ) determined by the 3-dB passband (parts of the electrical segment and the optical segment), the chromatic dispersion (CD) and influence of nonlinear optical effects (NOE) depending on the data transmission distance in the solution of the wavelength division multiplexed (WDM) system was evaluated, determining the optimal parameters for the development of a new hybrid broadband fiber optical amplifier, for high-speed FOTS solutions, ensuring the required BER of the received signal $\geq 1 \times 10^{-9}$.
4. A novel hybrid Raman-EDFA amplifier solution was developed, which combines the erbium-doped fiber and Raman effect amplification advantages, simultaneously performing optical signal amplification and chromatic dispersion (CD) compensation depending on the line length, capable of providing stable operation for in at least 16-channel DWDM communication system solution operated with 10 Gbit/s data transmission rate per channel, without exceeding the $BER \geq 1 \times 10^{-9}$ limit value of the received signal.

Practical significance of the Doctoral Thesis

1. In the Institute of Telecommunications of the Faculty of Electronics and Telecommunications of Riga Technical University, a new innovative erbium (Er^{3+})/ytterbium (Yb^{3+})-co-doped fiber optical amplifier model was developed capable of providing stable amplification in a WDM communication system solution in the C-band (1530–1565 nm) operation range.
2. In the Institute of Telecommunications of the Faculty of Electronics and Telecommunications of Riga Technical University, a new hybrid Raman-EDFA amplifier model has been developed capable of ensuring stable operation in at least a 16-channel DWDM communication system solution with a data transmission rate of 10 Gbit/s per channel, not exceeding the received signal $BER \geq 1 \times 10^{-9}$ limit value.

The results of the scientific research of the Doctoral Thesis have been applied in the implementation of the following project:

ERAF project “Development of efficient clad-pumped fiber optical amplifiers for telecommunication systems” No. 1.1.1.1/18/A/068.

Volume and Structure of the Doctoral Thesis

The Thesis is 123 pages long. It comprises an introduction, three chapters, conclusions and a bibliography.

Chapter 1 examines the factors influencing the SOPS, which need to be analyzed in order to conduct research on optical fiber amplifiers and their influencing parameters, thus taking into account the basic factors necessary for the simulative and experimental development of a hybrid broadband amplifier for WDM communication systems.

In Chapter 2, the physical foundations of the erbium-doped fiber amplifier EDFA, the physics of light amplification in a rare earth (erbium) doped fiber and the causes of noise are discussed, as well as information on the most common applications of EDFA is given. It also discusses the physical foundations of the Raman effect fiber amplifier, describes the mechanism

of light amplification with the help of induced Raman scattering, and discusses the noise evaluation of the Raman amplifier. The chapter concludes with a mention of common Raman amplifier applications.

Chapter 3 is the experimental part. In the experimental part, using the RSoft OptSim environment, as well as experimental work in the laboratory (experimental testing, development and measurement), the influence of fiber optic transmission line span and amplifier parameters on the quality of the transmitted signal in a wavelength-division multiplexed (WDM) system is investigated in order to determine the maximum distance, in which a quality signal can be transmitted using each of the types of amplifiers under investigation as well as both amplifiers together (using a hybrid amplifier).

At the end of the Thesis, based on the theoretical information and the results obtained in the experimental part, conclusions are made about the possibilities of using EDFA and Raman amplifier and their hybrid solution.

Approbation of Research Results

The main results of the Doctoral Thesis have been presented in 3 international scientific conferences and reported in 6 publications in scientific journals.

Reports at international scientific conferences

1. *Photonics and Electromagnetics Research Symposium, PIERS 2023 – Proceedings*, K. Zakis, S. Spolitis, T. Salgals, L. Gegere, **M. Parfjonovs**, D. Prigunovs, V. Bobrovs, A. Supe, “*Experimental Characterization of Signal Gain Evolution in Cladding-pumped Doped Fiber Amplifier*”, 3–6 July 2023.
2. *Photonics and Electromagnetics Research Symposium, PIERS 2023 – Proceedings*, D. Prigunovs, P. Morevs, **M. Parfjonovs**, T. Salgals, R. Kudojars, V. Bobrovs, “*Performance Analysis of Hybrid Raman-EDFA Amplifier in WDM Transmission Systems*”, 3–6 July 2023.
3. *Progress In Electromagnetics Research Symposium – Fall, PIERS – FALL 2017*, V. Dilendorfs, **M. Parfjonovs**, A. Alsevska, S. Spolitis, V. Bobrovs, “*Influence of Dispersion Slope Compensation on 40 Gbit/s WDM-PON Transmission System Performance with G.652 and G.655 Optical Fibers*”, 19–22 November 2017.

Publications in scientific journals

1. Zakis, K., Spolitis, S., Salgals, T., Gegere, L., **Parfjonovs, M.**, Prigunovs, D., Bobrovs, V., Supe, A. “*Experimental Characterization of Signal Gain Evolution in Cladding-pumped Doped Fiber Amplifier*,” 2023 Photonics & Electromagnetics Research Symposium (PIERS), Prague, Czech Republic, 2023, pp. 754–758, DOI: 10.1109/PIERS59004.2023.10221551
2. Prigunovs, D., Morevs, P., **Parfjonovs, M.**, Salgals, T., Kudojars, R., Bobrovs, V. “*Performance Analysis of Hybrid Raman-EDFA Amplifier in WDM Transmission Systems*,” 2023 Photonics & Electromagnetics Research Symposium (PIERS), Prague, Czech Republic, 2023, pp. 1787–1791, DOI: 10.1109/PIERS59004.2023.10221537
3. Pavlovs, D., Bobrovs, V., Alsevska, A., **Parfjonovs, M.**, Ivanovs, G. “*Investigation of Power Efficiency Changes in DWDM Systems Replacing Erbium-Doped Amplifiers by Semiconductor Optical Amplifiers*,” *Latvian Journal of Physics and Technical Sciences*, vol. 59, no. 1, 2022, pp. 44–52. DOI:10.2478/lpts-2022-0005

4. Zvirbule, K., Matsenko, S., **Parfjonovs, M.**, Murnieks, R., Aleksejeva, M., Spolītis, S. “*Implementation of Multi-Wavelength Source for DWDM-PON Fiber Optical Transmission Systems*,” Latvian Journal of Physics and Technical Sciences, vol. 57, no. 4, 2020, pp. 24–33. DOI:10.2478/lpts-2020-0019
5. Pavlovs, D., Bobrovs, V., **Parfjonovs, M.**, Alsevska, A., Ivanovs, Ģ. “*Evaluation of Signal Regeneration Impact on the Power Efficiency of Long-Haul DWDM Systems*”, Latvian Journal of Physics and Technical Sciences, vol. 54, no. 5, 2017, pp. 68–77, DOI: 10.1515/lpts-2017-0035
6. Dilendorfs, V., **Parfjonovs, M.**, Alsevska, A., Spolitis, S., Bobrovs, V. “*Influence of Dispersion Slope Compensation on 40 Gbit/s WDM-PON Transmission System Performance with G.652 and G.655 Optical Fibers*,” 2017 Progress in Electromagnetics Research Symposium – Fall (PIERS – FALL), Singapore, 2017, pp. 598–604, DOI: 10.1109/PIERS-FALL.2017.8293207

INTRODUCTION

Today, the volume of transmitted data is growing rapidly. Ericsson analysts predict an increase in mobile data from 51 EB in 2020 to 236 EB in 2026, of which 54 % will be 5G data flows [1].

In addition, the optical infrastructure is very widespread, and wide bandwidths are available, making it easy to create new systems. The development of new passive optical network (PON) standards involves coexistence with historical standards, thereby accelerating the transition to higher data rate networks [2].

The optical signal amplifier is an integral part of the set of elements of modern fiber optic transmission systems (FOTS). The range of applications for optical amplifiers is wide, ranging from low-cost, short-distance access networks to regional networks and long-distance intercontinental submarine networks. The renewed demand for higher bandwidth in fiber optic transmission systems influences the design of amplifiers. The development of wavelength division multiplexing (WDM) systems with a channel data transmission rate of 100 Gbit/s and more is underway. The need to meet the demands of these high transmission rate systems against higher capacity existing fiber optic and optical wavelength switching equipment requires more complex modulation and demodulation formats capable of encoding multiple bits per symbol and often incorporating differential or coherent detection. In general, such modulation formats increase the robustness of the system against chromatic dispersion (CD), polarization mode dispersion (PMD) and filtering distortions but place additional demands on the noise parameters of optical amplifiers due to their sensitivity to nonlinear signal distortions and increase demands on optical signal-to-noise (OSNR) relationship.

On the other hand, the characteristics of optical amplifiers, such as the spectrum of the amplification factor, its dependence on the channel density, saturation and dynamic impulse response, as well as the optical noises additionally introduced by the amplifier, impose restrictions on the development, construction and operation of transmission systems.

In recent decades, amplifier development has been driven by four main trends. The amplifier should have a wide optical gain bandwidth to work effectively in systems with a large number of channels. The optics and high-speed electronic components must ensure fast performance in dynamic networks. The trends of cost reduction and standardization of amplifier modules are also decisive. In response to the exponentially growing amount of data to be transmitted, networks are being built using dense wavelength division multiplexing (DWDM). Commercial networks use up to 160 channels with 50 GHz spacing in C- and L-bands. However, most networks use C-band for data transmission. Some time ago, fixed point-to-point (P2P) WDM systems were widespread. However, the rapid data volume growth led to a general reorientation towards dynamic optical networks. All new urban, regional and long-distance network solutions include devices based on the reconfigurable optical add-replace multiplexer (ROADM) principle for dynamic optical switching and are already widely used in the networks of large and regional telecommunications service providers. Therefore, the design of the amplifiers must meet the high-speed performance requirements of dynamic optical communication systems.

On the other hand, amplifier prices have significantly decreased over the past 10 years. This was due to reductions in the cost of pump lasers, erbium fiber and other components, and labour. The expansion of the supply of amplifiers in the market led to the pseudo-standardization of amplifier parameters. Changes in manufacturing approaches and amplifier designs have

contributed to the shift to modular amplifiers. Further changes in production and market expansion make it necessary to create standards in the field of amplifier production [3].

Erbium-doped fiber amplifiers and Raman fiber amplifiers are more common in modern networks. Long and long-distance networks use a hybrid solution consisting of EDFAs and Raman amplifiers.

Since its development in 1987, the erbium-doped fiber amplifier EDFA has revolutionized the field of telecommunications. Today, EDFA is considered a well-developed technology. One of its typical applications is ROADM, where the optical amplifier is an essential component. The ability to transmit optical channels using ROADM allows operators to reduce the cost per wavelength in the optical network. The gain can be obtained in any desired band with a Raman amplifier. Still, the gain can be given a smoothed form when the optical pumping is carried out at several wavelengths simultaneously. The spectral flexibility of the Raman amplifier is one of its main characteristics and advantages [3].

This study examines the most important working principles, features and limitations of EDFA and Raman fiber amplifier, and their role in fiber optic transmission systems. In the experimental part, when simulating a WDM transmission system, the influence of amplifiers and system parameters on the signal gain is investigated by simulating an EDFA and a Raman amplifier in a line separately, then a hybrid solution consisting of an EDFA and a Raman amplifier together in one transmission line span.

GENERAL DESCRIPTION OF THE RESEARCH

Chapter 1

In this chapter, the analysis and evaluation of the factors influencing the WDM's data transmission and the principles of the WDM communication system were studied.

Optical signal amplifiers are an integral part of FOTS solutions. The most common are erbium-doped fiber amplifiers EDFA and fiber Raman amplifiers. Raman fiber amplifiers based on dispersion-compensated fiber (DCF) are a potential application in future long-haul high-power fiber optic transmission systems FOTS. Hybrid Raman erbium fiber amplifiers (Raman-EDFA) are also available to improve the optical signal-to-noise ratio (OSNR) performance in optical transmission systems. This chapter analyzes the influencing factors and indicators of SOPS data transmission, which are necessary to justify the results obtained during the experimental development of the hybrid wideband optical amplifier and analyze all the aforementioned influencing factors.

Section 1.1 analyzes the classification and operating principles of the WDM communication system. Considering that there are other communication systems, FOTS is superior to them in terms of its features and capabilities. This is significantly influenced by the fact that optical fiber has a small attenuation compared to other materials used in data transmission. Optical fibre's low introduced attenuation ensures data transmission over much longer distances. On the other hand, a high throughput capacity of optical fiber makes it possible to transmit information at much higher speeds. The optical fiber is not affected by the adjacent modulated optical signals and is not subject to weak electromagnetic interference [4], [5].

The transmitter uses a radiation source, a modulator, and a radiation input device in an optical fiber. A laser diode is used as a radiation source. The function of the modulator is to change the amplitude, phase or polarization state, which is defined according to the required information transmission rate. The single-mode optical fiber (SMF) is basically used in the modern optical line segment. Of course, there are also solutions in which multimode fiber is used.

Various technologies are needed and used to increase the amount of data transmission: (1) wavelength division multiplexing technology (WDM); (2) time division multiplexing technology (TDM); and (3) space division multiplexing (SDM). WDM enables the simultaneous transmission of multiple channels over a single optical fiber [6], [7], [8]. The basic idea of TDM is to divide the bitstreams of the channels to be transmitted – to assign the bits of a specific channel the corresponding time interval and to transmit these multichannel bitstreams through a high-speed line. SDM technology is based on increasing the number of channels using multi-core optical fibers (MCF). WDM is the most common of all three technologies mentioned. SDM has not been fully explored and, for now, cannot replace existing fibers. The effect of inter-channel crosstalk characterizes WDM communication systems – in a given channel, the signal of other channels is represented as noise and thus shows the deterioration of transmission quality. The central elements of a WDM system are optical multiplexers/demultiplexers, as they combine/split spectral channels – in effect, performing passive routing by wavelengths [9].

All channel wavelengths of a WDM communication system are spaced with a certain inter-channel interval. According to the free spectral range of the interchannels, WDM communication systems are classified into coarse wavelength division multiplexing (CWDM)

communication systems and dense wavelength division multiplexing communication systems (DWDM). CWDM communication systems operate at wavelengths from 1271 nm to 1611 nm. The recommended inter-channel interval in the ITU-T G694.2 recommendation is 20 nm (2500 GHz), the channel arrangement of DWDM communication systems depends on different inter-channel intervals: 12.5 GHz, 25 GHz, 50 GHz and 100 GHz (recommended channel placement is specified in ITU-T G694.1 recommendation). With an inter-channel interval of 0.8 nm or 100 GHz, 80 channels can be realized in each wavelength range. DWDM communication systems with a channel spacing of 50 GHz and less are also called high-density wavelength division multiplexing communication systems (HDWDM) and allow multiplexing around 128 channels and more [10], [11].

There are three different types of optical signal recovery:

1R – optical signal amplification. This type of optical signal restoration is based on adding optical power without affecting the shape or synchronization of the optical signal.

2R – optical signal amplification and shape restoration, time interval length is not restored (synchronization).

3R – optical signal amplification, shape restoration and synchronization restoration. In addition to amplification and reshaping, the original signal synchronization (original cycle length) is also restored [9], [12], [13].

Section 1.2 analyzes nonlinear optical effects (NOEs) in fiber optical communication systems. The chapter analyzes the optical fibers and their NOEs, as well as their impact on the operation of optical communication systems. Nonlinear effects in fiber optics are similar to nonlinear effects in other physical systems (mechanical and electronic): they change the properties of the fiber and cause the generation of parasitic harmonics at frequencies equal to a linear combination of the fundamental frequencies of the system. As a result, the optical characteristic curves of the medium (polarization, refractive index, absorption coefficient) become functions of the electric field intensity of the light wave, and the polarization of the medium becomes nonlinearly dependent on the field intensity, but waves with different frequencies and propagation directions influence each other [14]. In an optical fiber, NOE appears already at powers from 1 W to 100 W. First of all, since the light propagates through the interior or core of the fiber, even at a small light intensity, it is quite significant in relation to the cross-sectional area of the fiber (it is the intensity that is important for NOE). Second, light propagates without defocusing (no change in cross-sectional area) over arbitrarily long distances. Various optical phenomena affect the propagation of light in optical fiber. These phenomena are divided into two large groups. The first one combines optical properties that do not depend on light intensity and only quantitatively changes the transmitted optical signal. The most important of them is the decay of the optical signal and the broadening of the short light pulses due to the optical fiber's dispersion, which is called linear optics. The second is nonlinear optics, which looks at the propagation of light in a substance whose optical properties change under the influence of light and studies NOE – optical phenomena caused by the nonlinear dependence of the polarization of the environment on the intensity of the electric field of light.

In **Section 1.3**, the criteria for evaluating the quality of the received signal of the fiber optic transmission system is carried out. Bit error rate (*BER*) measurements are often performed as a final quality acceptance test for newly constructed fiber optic transmission systems. *BER* is useful for testing existing transmission systems. Typical *BER* threshold values range from 1×10^{-9} to 1×10^{-13} [16], [18]. These threshold values vary depending on the organization, service

provider or transmission system. For example, ITU-T standards G.957 and G.984.2 define that PON systems use a threshold value of $BER < 1 \times 10^{-10}$ [19], [20], while other sources [16] and [17] mention that using $BER < 1 \times 10^{-9}$, as the sensitivity of optical receivers is often defined at this BER .

The received signal quality factor (Q-factor) is another system performance quality evaluation parameter that can be used as an alternative to BER testing. The Q-factor is defined as the ratio of the average photodiode current between the sensed “1” bit state and the “0” bit state divided by the sum of the standard deviation of the sum of the noise currents of the two conditions [16]–[18].

The signal parameters that can be obtained from the eye diagram can be divided into two groups: amplitude-related parameters and time-related parameters. Amplitude parameters are [15]: average power, logical “1” and “0” levels, eye amplitude and aperture height, fluctuations of logical “1” and “0” levels and the ratio of high and low power levels, which characterize the optical signal modulation depth. An eye diagram shows the summary picture of several bit periods of the measured discrete signal superimposed on each other. Respectively, the mesh diagram is created by overlapping bits many times, one on top of the other [16].

To understand the operation of dense wavelength division dense passive optical network systems (WDM-PON), it is necessary to look at the frequency spectrum available to them, which can be divided into several bands. Currently, light wavelengths from 660 nm to 1600 nm are used for information transmission in fiber optics. Single-mode optical fibers use a passband from 1260 nm to 1675 nm (corresponds to the O, E, S, C, L, U bands mentioned in the ITU-T G.694.2 recommendation). Generally, 58.95 THz or 415 nm passband can be used in single-mode optical fiber transmission systems. In WDM systems, the usable frequency spectrum is divided into six bands. These bands recommended by the International Telecommunication Union (ITU) are summarized in Table 1 [18], [21].

Table 1

WDM Frequency Bands Defined by the ITU-T G.694.2 Recommendation [22], [23]

Band definition	Band type/encryption	Wavelength range, nm
O	Original	1260–1360
E	Extended	1360–1460
S	Short wavelength	1460–1530
C	Conventional	1530–1565
L	Long wavelength	1565–1625
U	Ultra long wavelengths	1625–1675

Chapter 2

Optical amplifiers are classified according to the nature of the amplification process [21]:

1) amplifiers, where the gain is obtained using the linear properties of the material (semiconductor optical amplifiers (SOA) and amplifiers based on rare-earth element-doped fibers (x DFA));

2) amplifiers whose operating principle is based on the nonlinear properties of the material (Raman optical amplifiers, Brillouin optical amplifiers and parametric amplifiers (FOPA)).

The second principle by which optical amplifiers are classified is the gain medium:

- 1) amplifiers using semiconductor material SOA;
- 2) amplifiers that are created based on optical fibers.

Further in this chapter, each type of the above-mentioned optical amplifier will be discussed in more detail, and their main advantages and disadvantages will be analyzed.

Section 2.1 evaluates the construction and operating principle of the EDFA amplifier as well as its use in FOTS solutions. Doped fibre optical amplifiers are the most widely used optical amplifiers. In amplifiers of this type, silica fiber is doped with rare earth elements during manufacturing to create a two-, three- or four-level system capable of efficient pumping. Such amplifiers can use 14 rare earth chemical elements with atomic numbers between 58 and 71. Ions of rare earth elements such as erbium, holmium, neodymium, samarium, thulium and ytterbium could be used to make doped fiber amplifiers that operate in the wavelength range of visible light up to infrared radiation [24]. The most commonly used rare earth element is erbium, because erbium-doped fiber optical amplifiers in EDFAs operate in the C-band (1530–1565 nm), where the minimum of the attenuation curve of silica fibers is observed [24]. EDFA optical amplifiers are also designed to work in the L-band (1565–1625 nm) [25]. These are often referred to as “shifted gain” EDFAs, and such a shift of the gain spectrum is achieved by using fluoride and other elements in the fiber fabrication process [25].

A typical gain produced by an EDFA is around 30 dB, but a gain of 54 dB can also be achieved [27]. The more channels are transmitted in an optical fiber, the higher the excitation energy required. Different pumping schemes are used in EDFA amplifiers:

- 1) with direct pumping, it is able to provide a lower noise level at low input signal power and high gain;
- 2) with reverse pumping, less pumping radiation power is required to achieve amplifier saturation than forward pumping.

One of the network design problems is the choice of wavelength for the EDFA amplified pumping source – 980 nm or 1480 nm. Efficient pumping can be achieved with pumping radiation with a wavelength close to 980 nm or 1480 nm [24]. With 980 nm pumping radiation, achieving a higher level of population inversion is possible, allowing for a lower amount of amplified spontaneous emission (ASE) noise. So, from a noise point of view, it is better to use 980 nm pumping radiation. On the other hand, the quantum efficiency of the amplifier is higher at 1480 nm pumping because the difference in energy level between the pumping and amplifying radiation is negligible. So, with 1480 nm pumping radiation, a higher amplification factor can be obtained [26]. First, it is difficult to determine which will be preferred – high gain or low noise. It is also necessary to find a compromise, considering the system costs and the advantages and disadvantages of each wavelength [28], [29]. The gain efficiency is measured in dB/mW and is defined as the tangent of the angle formed by the tangent to the horizontal axis of the plot of the gain versus pump power from the coordinate origin. Table 2 compares these two wavelength parameters [28], [29].

Table 2

Comparison of Pumping Source Wavelengths [5], [28]

Parameter	Wavelength, nm	
	1480	980
Laser diode	InGaAsP/InP	InGaAs/APD
Amplifier efficiency*, dB/mW	6.3	11
Noise level, dB	~ 5.5	3–4.5
Output efficient power**, dBm	+ 20	+5
Pumping band, nm	20 (1470–1490)	narrow, 2 (979–981)
Splitting	hard	easy
Output power, mW	50–200	10–20
* At similar EDF fiber length.		
** Depends on the pump power.		

In Section 2.2, the application and evaluation of the Raman amplifier is performed. One application of the Raman effect is the Raman optical amplifier. There are discrete and distributed Raman amplifiers. Discrete amplifiers are a separate module that performs amplification at an end of the line section. For split amplifiers, the amplification does not take place in a separate module with a wound fiber but in the line itself. The gain efficiency of Raman amplifiers is lower at low input signal power levels and increases with increasing signal power. This is because stimulated Raman scattering is a coherent energy transition process.

Consequently, a relatively powerful signal will be amplified more efficiently than noise with a much lower power level [30]. Such coherent amplification can lead to an improvement in the signal-to-noise ratio (SNR) at the output of the amplifier and to negative values of the introduced noise figure, indicating that the signal is amplified more efficiently than the noise, and its power gain is more significant [32]. However, providing Raman amplification at low input signal power levels requires powerful pumping radiation sources with an optical radiation power close to (or greater than) 1W [30], [31].

In Raman amplifiers, as in the case of EDFAs, forward, reverse, and bidirectional pumping schemes can be used. The phenomenon of Raman scattering is a swift process that takes place within a few femtoseconds.

Section 2.3 evaluates the application of semiconductor optical amplifiers (SOA) in communication system solutions. A semiconductor optical amplifier is an opto-electrical device, which, under certain operating conditions, can amplify the light propagating through it. This device uses the phenomenon of stimulated emission to provide optical signal amplification. The pumping current is the external energy flow that ensures the achievement of population inversion. The carriers of this current occupy a position in the conduction zone of the active layer, leaving “holes” in the valence zone [33]. Three transition mechanisms are possible in semiconductor materials: spontaneous emission, stimulated emission, and stimulated absorption.

The energy level spontaneous lifetime for semiconductor amplifiers ranges from a few nanoseconds to a few hundred picoseconds [33]. Therefore, there is always a probability that an electron in the conduction band will not come into contact with a photon of the amplified signal during the lifetime of the excited state and, therefore, as a result of spontaneous emission,

will produce a photon with a random propagation direction, wavelength and phase. Because of this, a large amount of amplifier noise appears in the signal. This additive noise is an undesirable part of the amplification process, but its occurrence cannot be completely avoided [17]. These spontaneously generated photons not only introduce noise over a wide frequency range but also reduce the level of population inversion, which negatively affects the achievable gain level. Spontaneous emission is a direct consequence of amplification, making noiseless semiconductor amplifiers impossible.

Semiconductor amplifiers are mainly classified into two types: Fabry-Perot (FP-SOA) and travelling wave amplifiers (TW-SOA). Travelling wave semiconductor amplifiers are amplifiers where reflection is a tiny fraction of the estimated signal energy that is reflected as it propagates through the TW-SOA, which is 0.01 %. Various anti-reflection coatings can also be used to obtain semiconductor amplifiers with a reflection coefficient of less than 10⁻⁵. TW-SOA is less sensitive to pumping current fluctuations, temperature changes, and amplification signal polarization than FP-SOA [33].

The advantages of SOA are high gain (~ 30 dB), simple construction and broad gain spectrum. The spectrum width is usually between 40 nm and 50 nm, but there are also SOA amplifiers with a broader range of 60 nm and more. Disadvantages include high ASE noise, high insertion loss (~ 10 dB), polarization sensitivity and distortion of the signal spectrum.

Section 2.4 evaluates the use of the Brillouin optical amplifier in communication system solutions. The gain produced by Brillouin amplifiers can be used to amplify weak optical signals whose frequency is shifted relative to the frequency of the pumping radiation by an amount equal to the Brillouin shift. Semiconductor lasers are used to pump Brillouin amplifiers because their emission frequency band is much narrower than the Brillouin amplification band. Brillouin amplifiers can provide 30 dB of gain at pump radiation power of less than 10 mW, which is a considerable advantage compared to other optical amplifiers. The Brillouin amplification spectrum is narrower than 100 MHz, and the frequency difference between the pumping and amplifying signal must correspond to the Brillouin shift with an accuracy of up to 10 MHz. For this reason, Brillouin optical amplifiers are not used in fiber optic transmission systems to amplify optical signals. They can be used for other purposes, for example, to improve the sensitivity of the receiver by selectively amplifying the signal of a certain frequency before detection, or as tunable narrowband optical filters for channel selection in a dense multichannel system with a transmission rate of a few tens of megabits per second in the channel [17], [25].

Chapter 3

In accordance with the stated goal of the DThesis, defined work tasks and proposed theses, this chapter describes and illustrates the results of the experimental part of the Thesis and their sequential descriptions.

Cascade connections of different optical amplifiers are considered as a combined solution of amplifiers (hybrid amplifier). In order to obtain a higher gain with a lower amount of introduced noise and to expand the gain spectrum, combined solutions are created.

In the obtained hybrid solution, the gain created by the used optical amplifiers is summed [25], [34], [35].

The combined solutions used to amplify the optical signal are classified into two primary groups:

1) wideband combined solutions (seamless and wideband hybrid amplifiers, SWB-HA), where different types of optical amplifiers are used to obtain the broadest possible amplification spectrum in combination with a lower amount of introduced noise;

2) narrow band hybrid solutions (e.g. narrow band hybrid amplifier, NB-HA), where different types of optical amplifiers are used to obtain higher gain at a higher optical signal-to-noise ratio (SNR).

In the case of wideband combined solutions, the typical gain spectrum is around 80 nm, while in the case of narrowband combined solutions, the typical gain spectrum is in the range of 30–40 nm. Narrowband solutions are usually applied in C or L wavelength bands, but in the case of broadband solutions, both bands can be used in parallel, thus forming a dual-band amplifier [25].

In **Section 3.1**, the influence of dispersion on the operation of the WDM communication system is evaluated. RSoft OptSim simulation software was used to implement the wavelength-division compressed WDM communication system experimentally. At this stage, the transmission rate was set to 40 Gbit/s per channel for all experimental and simulation models. The transmitter was built from 5 main elements: a data source; an RZ or NRZ coders; a continuous wave laser light source (CW); a Mach–Zehnder intensity modulator (MZM); and an optical bandpass filter (OBPF). The center frequencies of the channels, starting from channel 1 to channel 16, were determined from 192.4 THz to 193.9 THz. Operating channel frequencies were selected according to ITU-T G.694.1 recommendations. The receiver for all channels was constructed using three elements – an optical bandpass filter OBPF, a second-order optical Bessel filter, a PIN photodiode and a fourth-order electrical low-pass filter (LPF). The FOTS transmission line was constructed from SMF (G.652) or NZDSF (G.655) optical fiber span; dispersion compensated fiber (DCF) for CD compensation and Bragg grating (FBG) for dispersion slope (CD_{SL}) compensation. The FOTS transmission line splitter and combiner with the transmitter and receiver optical filters formed an array waveguide grating (AWG) multiplexer and demultiplexer.

FOTS's transmission line length was 50 km for both RZ and NRZ modulated signals using SMF. Accordingly, a dispersion compensation module (DCM) and amplifiers were added to compensate for the accumulated CD dispersion values and the attenuation (IL) introduced by the fibers in the optical line. Additional amplifiers were used to compensate for DCF insertion loss, the gain of which was the same as the insertion loss values of the DCF fiber span. A *BER* of less than 10^{-12} was defined to determine channel performance.

The location of the DCM was changed in FOTS with the aim of finding out how the location of the DCM would change the performance of individual channels in a 16-channel WDM system. The experimental simulation was initially performed on a 16-channel system with RZ line code format using DCF for pre-, post- and symmetrical CD compensation. In the continuation of the simulation experiment, the RZ line code was changed to the NRZ line code and the CD compensation simulations were repeated. The SMF was then replaced by the NZDSF, and the simulations were repeated. After all CD compensation simulations, an additional fiber Bragg grating (FBG) was added for CD_{SL} compensation.

First, the transmission line length of a 16-channel WDM system with a data transmission rate of 40 Gbit/s per channel was determined without CD and CD_{SL} compensation. Using the RZ line code, the maximum transmission line length was 3.0 km with SMF (accumulated CD value was 48.0 ps/nm), but with NZDSF, the transmission line length was 6.9 km (accumulated

CD value was 27.6 ps/nm). The worst result was recorded in channel 11 (193.4 THz), where the *BER* value with SMF was 4.7×10^{-13} and the *BER* value with NZDSF was 9.6×10^{-13} , respectively. The specified *BER* threshold ($BER < 10^{-12}$) was not exceeded. The maximum obtained transmission line length using the NRZ line code with SMF was only 2.4 km (accumulated CD value 38.4 ps/nm), but with NZDSF this length reached 10.2 km (accumulated CD value 40.8 ps/nm). The worst channel performance in SMF and NZDSF was observed in several defined channels. Using SMF fiber, the worst result was observed in channel 13, where the *BER* was 1.5×10^{-13} , while NZDSF was observed in channel 12, where the *BER* was 7.0×10^{-13} . The total accumulated CD value was 800 ps/nm for a 16-channel WDM system with a data transmission rate of 40 Gbit/s per channel using a 50.0 km SMF. DCF was used for CD compensation, and an additional fiber Bragg grating (FBG) was added to FOTS for CD_{SL} compensation.

In **Section 3.2**, the four-wave interaction (FWM) effect is used to create spectrally efficient SOPS solutions. This section investigates the use of the FWM optical effect to create a multi-wavelength light source for the use in 16-channel DWDM-PON communication system. An experimental simulation model with an FWM multiwavelength light source for the DWDM-PON transmission system was developed in RSoft OptSim simulation software environment. The power of the pumping lasers was varied between + 15 dBm and + 30 dBm. Different span lengths of high nonlinearity fiber (HNLf) up to 2 km were also investigated. A fourth frequency was generated as a result of the FWM process. In order to effectively influence the FWM effect in the HNLf fiber, the following HNLf parameters were determined: effective area $11.6 \mu\text{m}^2$, zero dispersion wavelength 1552.32 nm, and nonlinear coefficient $11.50 (\text{W} \times 1)^{-1}$. The center frequencies of the CW laser light sources used in this study were 193.1 THz (1552.524 nm) and 193.15 THz (1552.123 nm), and the attenuation factor for generating up to 16 carriers in the HNLf fiber was 0.8 dB/ng [36]. The parameters of the waveguide array AWG multiplexer and demultiplexer used in DWDM-PON systems were as follows: the inter-channel interval was 50 GHz, the optical 3-dB bandwidth was 16.5 GHz, and the center frequency of the lowest channel of the waveguide array AWG multiplexer and demultiplexer was varied depending on the number of channels used: 1) for 4 channels – 193.05 THz; 2) for 8 channels – 192.95 THz; 3) for 16 channels – 192.75 THz. The optimal pumping power of the CW laser light source and the length of the HNLf span were determined experimentally using a simulation model. These parameters were found by evaluating the AWG output's optical spectrum, considering the generated carriers' lowest power variation, which did not exceed the range of 3 dB.

FWM multi-wavelength light sources were experimentally configured, the parameters of which varied depending on the number of channels used in the communication system. Experimental simulation models of up to 8-channels, 4-channels, and 16-channels DWDM-PON transmission system with a defined FWM multiwavelength source was developed in mathematical simulation environment.

In addition to the waveguide array AWG multiplexer and demultiplexer, an optical element (optical attenuator) was added to simulate the optical attenuation, corresponding to the available solution of the AWG multiplexer and demultiplexer. Data transmission channels with a data transmission rate of 10 Gbit/s per channel, i.e. each transmitter Rx, consists of a data source, an NRZ coder, and Mach-Zehnder intensity modulator MZM. During the study, the number of data transmission channels varied from 4 to 16 channels. According to ITU-T G.652, SMF fibre was used as part of the optical network segment. The fiber length was 20 km, the attenuation

and the measured channel power levels was in channel 4, which was 0.5 dBm. However, in an 8-channel system, the average peak power per channel was 0.7 dBm, where the difference between the worst channel was 1.3 dBm (for channel 1). In the 16-channel DWDM-PON transmission system, the average channel peak power was 2.8 dBm, and the difference between the calculated average channel peak power and the measured channel peak power was 2.9 dBm (for channel 4). The obtained values are acceptable as they fall within the range of 3 dBm. Figure 2 shows the spectrum for a DWDM-PON transmission system with 4 channels (a), 8 channels (c), 16 channels (c) after AWG multiplexer; 4 channels (b), 8 channels (d), and 16 channels (f) after the transmission line section. Figure 3 shows the eye diagrams of the received signal in a 4-channel (a), 8-channel (b), and 16-channel (c) DWDM-PON transmission system with an FWM multiwavelength light source.

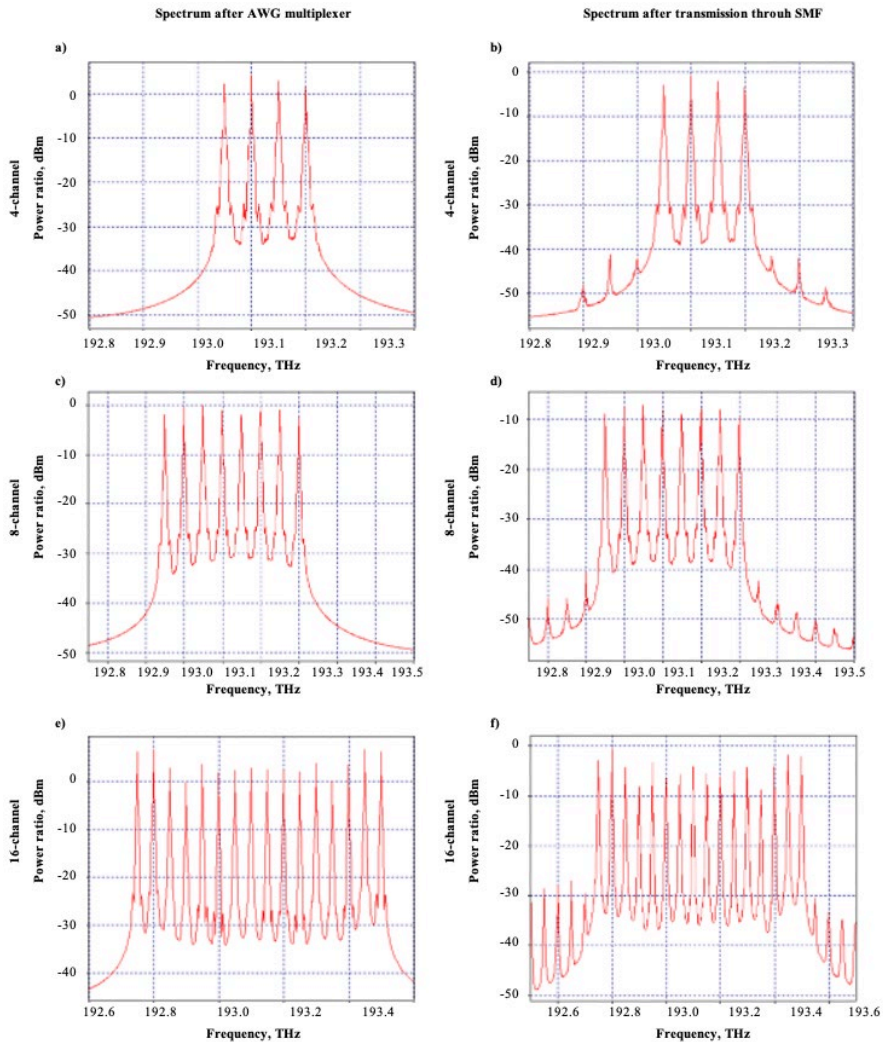


Fig. 2. The output spectrum of the DWDM-PON transmission system with FWM multiwavelength source – a) 4-channel, c) 8-channel, e) 16-channel after the AWG multiplexer, and b) 4-channel, d) 8-channel, f) 16-channel after the 20 km long SMF transmission line.

As can be seen in Fig. 3, the quality of the eye diagram deteriorates due to increased dispersion and nonlinear effects when a higher number of channels is generated from 4 channels to 16 channels for the FWM multiwavelength light source.

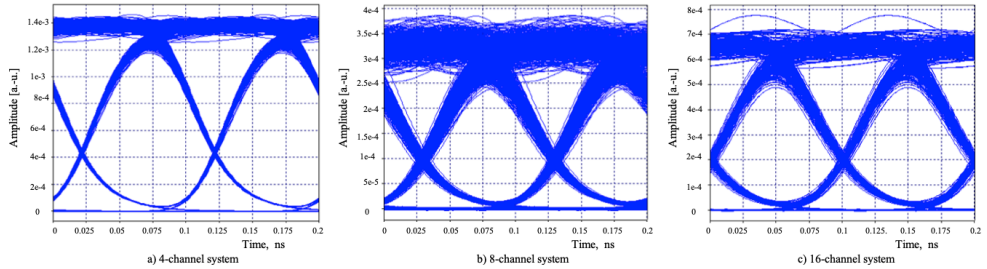


Fig. 3. Eye diagram of DWDM-PON transmission system with FWM multi-wavelength light source: a) 4 channels, b) 8 channels, and (c) 16 channels.

Table 3 shows the *BER* values of the received signal up to a 16-channel DWDM-PON transmission system, where the worst fixed channel of the 4- and 16-channel system solution is the fourth channel, and the first channel in the 8-channel system solution. However, the transmission lines are believed to perform well with low losses since the “eye” aperture is open in all cases, and the *BER* is below the threshold of 1×10^{-10} . According to the ITU-T G.984.2 recommendation, the *BER* value of received signals for fiber optical transmission systems with a bit rate of 10 Gbit/s per channel should be less than 1×10^{-10} [20].

Table 3

BER of Received Signals for up to 16 Channels in the DWDM-PON Transmission system

	4 channels	8 channels	16 channels
<i>BER</i> value for the worst performing system channel (20 km long SMF)	1×10^{-40}	2.5×10^{-23}	6.5×10^{-14}

An experimental study investigated up to 16-channel DWDM-PON transmission system with FWM multi-wavelength source. The FWM effect was used to generate multi-carrier (multi-wavelength) optical carriers for a 4-, 8- and 16-channel DWDM-PON transmission system. The first step was to find the optimal CW pump laser power and the length of the HNLf fiber to generate the FWM carrier, which could be further used for data modulation and transmission. As a result of the study, it was found that for a DWDM-PON transmission system with a data transmission rate of 10 Gbit/s per channel, using a 50 GHz channel spacing, the CW pumping power level of the continuous wave laser light source for both light sources in the case of a 4-channel system was + 20 dBm @ HNLf of 0.9 km length. In order to increase the number of channels of the DWDM-PON transmission system from 4 channels to 8 and 16, and generate more carriers, it was necessary to increase the power of the pumping CW laser light source. Thus, for the 8-channel system, the CW laser light source's CW power reached the output power level of the pumping source of 24.1 dBm, and the HNLf length reached 1.39 km. On the other hand, the 16-channel system was 26.3 dBm and 1.05 km, respectively. The SBS threshold must be considered to increase the number of FWM-generated carriers for a DWDM-PON system with 8 to 16 channels, otherwise, the output power of the carrier is uneven, and as a result, a

16-channel system cannot be created. The *BER* values and received signals eye diagrams were evaluated for the worst channel of the DWDM-PON system. Analyzing the received signal after transmission of a 20 km span through SMF, it was observed that in a 4-channel DWDM system, the worst channel *BER* value was 1×10^{-40} , while in an 8-channel system, the worst channel *BER* value was 2.5×10^{-23} , and in a 16-channel system, the worst performance the *BER* value of the channel was 6.5×10^{-14} .

Section 3.3 evaluates the effect of signal regeneration on DWDM solutions. This experimental study investigated the power efficiency of the three most widely used signal modulation formats in DWDM systems. The analytical model was developed in such a way that the signal detection error probability factor at the receiving node at a point-to-point (P2P) transmission distance of 2960 km would be lower than 1×10^{-3} . For this, the transmission reach for each defined parameter was defined with the help of simulation using RSoft OptSim software, and the system power consumption and efficiency were calculated using the obtained results. The influence of the signal regeneration process on the total system energy consumption was tested for each setting of the simulation. The results were presented as functions of the amount of transmitted data operating at different values of the inter-channel interval, which allows for tailoring the results in WDM implementations with various available spectrum bands.

This study provides a comparison of power efficiency values and DWDM setups operating at 10 Gbit/s NRZ-OOK, 40 Gbit/s NRZ-DPSK or 100 Gbit/s DP-QPSK transmission signals, and it is possible to fix the required power ratio. The results obtained within the research framework for the mentioned settings can be used in designing an energy-efficient DWDM system.

Based on relevant studies [37]–[39], power consumption values of transponders and 3R regenerators depending on modulation – non-return-to-zero line code with on-off manipulation (NRZ-OOK), non-return-to-zero line code with differential phase manipulation (NRZ-DPSK), and non-return-to-zero line code with quadrature phase manipulation (NRZ QPSK) – are summarized in Table 4.

Table 4

Power Consumption W of Transponders and 3Rs

Bit rate, Gbit/s	Modulation format	Consumer	Power, W
10	NRZ-OOK	TP/3R	34.0 (Typ)
40	NRZ-DPSK	TP/3R	85 (Max)
100	DP-QPSK	TP/3R	139 (Typ)

In the experimental study, the energy consumption values for each considered system implementation were evaluated using different inter-channel intervals based on the fact that cross-talk interference between channels is unique for each type of signal operating in the same frequency range. Since the purpose of this experiment is to evaluate the effect of regeneration on power efficiency and total energy consumption, it is therefore not worthwhile to analyze different systems using the same channel distribution. The lower limit of the frequency intervals for the experimental analysis was chosen based on the highest spectral efficiency that can be achieved, ensuring the fulfilment of the defined *BER* requirements. The upper limit was derived from the conditions when transmission volumes reached their maximum, meaning further

increasing the frequency limit would only lead to a decrease in spectral efficiency without any beneficial positive effect on energy consumption. Since this study considered different spectral efficiencies in different frequency intervals, the transmission reach became dependent on the inter-channel interval. The relationship between frequency interval or inter-channel interval, spectral efficiency (SE) and transmission reach is summarized in Table 5.

Table 5

Spectral Efficiency and System Reach at Different Channel Spacing Values

Channel spacing, GHz	SE, bit/Hz	Reach, km
10 Gbit/s NRZ-OOK		
12.50	0.80	160
18.75	0.53	1680
25.00	0.40	5700
31.25	0.32	8720
40 Gbit/s NRZ-DPSK		
50.00	0.80	160
56.25	0.71	240
62.50	0.64	560
75.00	0.53	960
87.50	0.46	1440
100.00	0.40	2080
112.50	0.36	2080
100 Gbit/s DP-QPSK		
31.25	3.20	160
37.50	2.67	400
43.75	2.29	1040
50.00	2.00	1360

Section 3.4 evaluates the power efficiency change in the DWDM communication system solution depending on the type of optical amplifier used. The experimental part of this subsection for defining settings and the methodology for collecting and processing information is similar to that described in the previous section. According to the objectives of this study, only input data and system parameters have been changed. In these simulations, the focus was more on the rationale for defining the parameters. First, the relationship of DWDM transmission with EDFA and SOA gains was simulated for several transmission distances using RSoft OptSim by WDM component technical data sheets and recent research results for specific SOA parameter definitions. The developed transmission system did not include forward correction code (FEC) schemes. Accordingly, the main goal of this simulation is to achieve a receiver Q-factor level of greater than 16 dB, which corresponds to a 1×10^{-9} bit error *BER* measured in the worst channel (central channel).

In this experimental simulation, the central wavelength was set to 193.0 THz instead of the standard 193.1. This was done to account for possible additional confounding, such as higher losses in the optical fiber [40].

The CW laser source light was split into four constant beams at a power level of 0 dBm, each of which was driven by 25 Gbit/s pseudo-random bit sequence (PRBS) generators using

amplitude modulators. 90° phase modulation was performed on two modulated optical beams, which, after phase modulation, combined two signals with orthogonal phases for further polarization modulation. All four optical signals were combined and transmitted through a bilateral optical Gaussian filter, i.e. a 3-dB bandwidth equal to 35 GHz.

The number of channels was determined by non-linear distortion statistical calculation [41], which showed that the effect of XPM on a given transmission channel against four subsequent channels reached ~ 97 % of the maximum possible. The generated and combined optical signals are then amplified by an EDFA amplifier model with a fixed optical output power of 14 dBm, introduced noise figure NF = 4.5, or by an SOA amplifier model with a signal gain of 8 dBm, introduced noise figure NF = 8 and 14 dBm typical saturation power (P_{sat}).

It should be noted that SOA performance can have two modes – static, assuming no gain fluctuations, and dynamic. The static mode can be found as follows (1) [42]:

$$h(t) = \ln(G_0) - \left[\frac{P_{in}(t)}{P_{sat}} \right] \cdot [e^{h(t)} - 1], \quad (1)$$

where $h(t)$ is SOA gain exponent; G_0 is SOA low signal gain; and $P_{in}(t)$ is SOA input power.

The main objective of this study was to evaluate the impact of replacing EDFA with SOA on energy efficiency level, taking into account the latest findings on SOA. Based on research aimed at evaluating the performance of SOA as an alternative low-cost gain component for DWDM systems in replacing EDFA with SOA and considering the latest findings on SOA, it was necessary to carry out the experimental simulation previously performed to find the best combination solution design for further research. To achieve this goal, the current study evaluated and compared the power efficiency levels in the proposed replacement scenario when the EDFA reinforced optical link where 86 channels of C-band is used. The total capacity was doubled by using SOA instead, providing 182 transmission channels due to the broader gain bandwidth. Both configurations used 100 Gbit/s DP-QPSK transmission signals separated by 50 GHz channel spacing.

In the first step of the simulation, it was shown that taking into account the correlation between the nonlinear distortion and the ratio of the input power $P_{in}(t)$ and the saturation power P_{sat} of the semiconductor amplifier, it was possible to adjust the transmission parameters so that the Q factor is greater than 16 dB in a 640 km long optical fiber line.

Next, energy efficiency levels were calculated based on the obtained results and the available parameters of the transmission system components. A comparison of the calculated values showed that the system with SOA gain required less energy for the transmission of one bit, and this difference became more significant for longer transmission distances – from 1.6 % to 12.6 %, respectively, 80 km and 640 km along the optical fiber lines. This proves that SOA and the relatively low cost of components could provide additional environmental and financial benefits.

It should be noted that since this is a first step to estimating the power consumption volumes for SOA-enhanced systems, several potentially critical system parameters, physical interference, and hardware availability and compatibility issues are beyond the scope of this study.

Section 3.5 describes the development of a new innovative erbium (Er^{3+})/ytterbium (Yb^{3+})-co-doped fiber optical amplifier and evaluation in FOTS. The main goal of this experiment is to investigate a solution for an optical amplifier based on a erbium (Er^{3+})/ytterbium (Yb^{3+})-co-doped fiber, i.e. to compare the gain changes of optical carriers depending on the span length of the -co-doped fiber (2–7 m), the output power of the multimode pumping source (0.6–2.0 W) and the operation wavelength (C-band (1530–1565 nm)). As a result, the “gain” is determined, and the operating band is based on the power stability of the optical carriers. Figure 4 shows the experimental scheme used for gain measurements of an innovative erbium (Er^{3+})/ytterbium (Yb^{3+})-co-doped fiber optical amplifier. The experimental setup consists of a erbium (Er^{3+})/ytterbium (Yb^{3+})-co-doped fiber, which is connected at both ends to a double-clad combiner/splitter providing the functionality of the pumping source and the input/output connection of the optical carriers. The rare-earth-doped inner part of the fiber is flower-shaped to achieve a light-focusing effect that promotes overlap between the multimode pumping source and the doped fiber core. The primary driver of the amplification process is the concentration of rare earth elements, which is very important for the combination of such amplifiers. The core of the fiber used in this solution is doped with erbium and ytterbium, and this was determined as an atomic percentage of 0.06 % and 1.21 %, respectively [43]. It is a Yb^{3+} to Er^{3+} ratio of 20.17, which shows that Yb^{3+} plays the leading role in absorbing the pumping light and transferring this energy to the Er^{3+} ions. The corresponding absorption and emission cross-sections calculated from the absorption measurements are shown in Fig. 5. These data were fed into the model to determine the initial range of fiber lengths and pump power levels that could support broadband amplification in C-band [44].

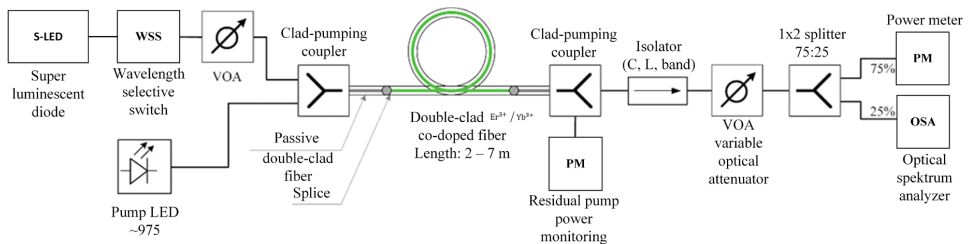


Fig. 4. Experimental scheme of innovative erbium (Er^{3+})/ytterbium (Yb^{3+})-co-doped fiber optical amplifier for channel gain measurements.

On the input side of the experimental setup, there is a high-power pumping source (multimode pumping source) with a central wavelength of 975 nm and a bandwidth of 6 nm, which is maintained at 30 °C with a thermoelectric cooler (with a Peltier thermocontroller on a platform matching the laser diode) to prevent its output wavelength and power fluctuations. The input signal is generated by filtering the light produced by a superluminescent light-emitting diode (S-LED) with a –10 dB optical output power and an optical signal bandwidth between 1526 nm and 1630 nm. A wavelength selective switch (WSS) filters the S-LED and generates a spectrum limited to the C-band, which, in turn, consists of 48 channels with 100 GHz inter-channel spacing and a 37.5 GHz bandwidth. This optical carrier signal containing a 48-channel interpretation is used for all future studies, and its power is regulated by a variable optical attenuator (VOA).

In the experimental solution, a double-clad fiber splitter/combiner on the output side of the doped fiber is used to separate the pump light from the amplified signal. A thermal power sensor monitors the unabsorbed pumping light. Next, the amplified optical signal is split by an optical power splitter (50/50 % splitting ratio) between a photodiode-based optical power meter (PM) and an optical spectrum analyzer (OSA), which are used for gain measurements of each individual channel, respectively.

To test the amplifier, the following three parameters were controlled and varied within the given ranges:

- 1) $\text{Er}^{3+}/\text{Yb}^{3+}$ co-doped fiber length from 2 m to 7 m;
- 2) the optical power level of the signal of optical carriers from -27 dBm to -10 dBm (in the channel);
- 3) the 975 nm pump source output optical power level is from 0.6 W to 2.0 W.

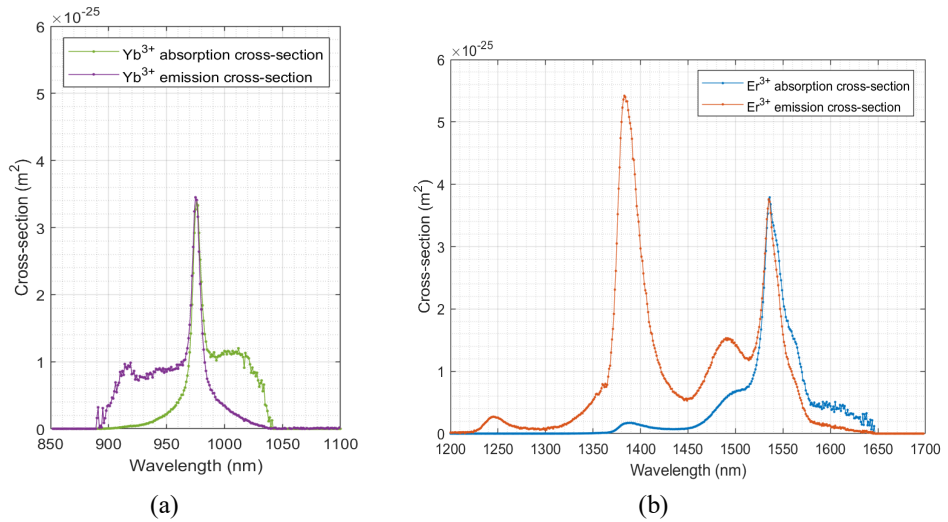


Fig. 5. Absorption and emission cross-section spectra calculated from absorption measurements for (a) Yb^{3+} and (b) Er^{3+} ions.

In Fig. 6 (a), the pump source is set to the lowest output power level of 0.6 W, which produces a significant peak gain at 1536 nm, achieving a gain of 34 dB using a 2 m double-clad $\text{Er}^{3+}/\text{Yb}^{3+}$ doped fiber span with an optical carrier input power of -27 dBm. If the span of the erbium (Er^{3+})/ytterbium (Yb^{3+}) -co-doped fiber increases, this peak decreases, the second peak at 1544 nm becomes more prominent, and the gain at longer wavelengths increases. For a 7 m long erbium (Er^{3+})/ytterbium (Yb^{3+}) -co-doped fiber, a third peak appears at 1563 nm, but the peak at 1544 nm is reduced. This results in a relatively linear gain between the two wavelengths mentioned above.

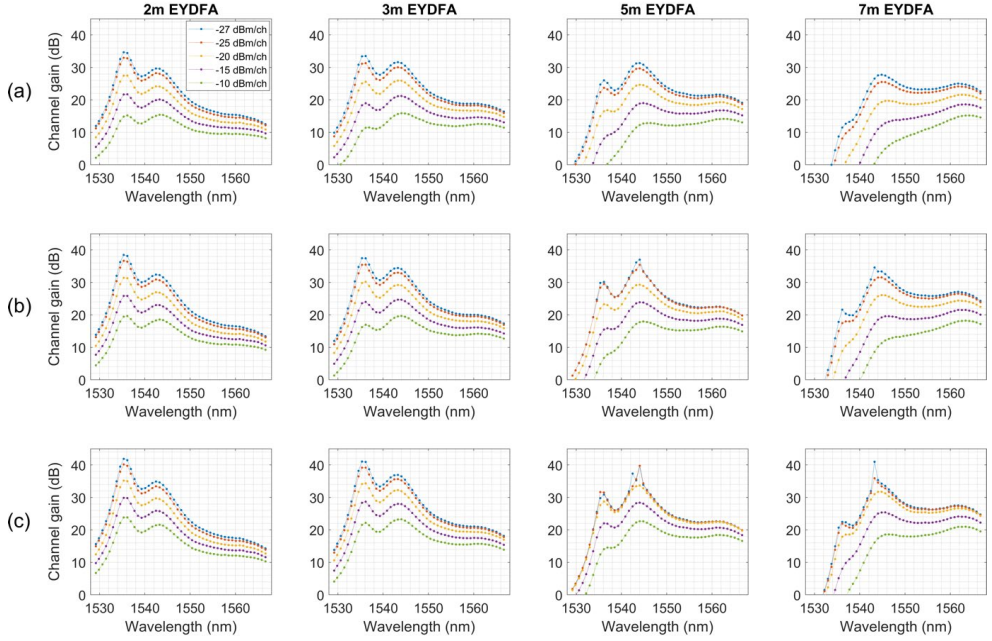


Fig. 6. Channel gain evolution with erbium (Er^{3+})/ytterbium (Yb^{3+})-co-doped fiber length between 2 m and 7 m at input signal power of -27 to -10 dBm per channel with 976 nm multimode pump laser power set to (a) 0.6 W, (b) 1.0 W, (c) 2.0 W.

If the pumping power is increased from 0.6 W to 1.0 W, Fig. 6 (b), the gain is increased for all channels, but the peak gain becomes even more prominent. However, at a span length of 5 m erbium (Er^{3+})/ytterbium (Yb^{3+})-co-doped fiber, the input carrier optical signal in the -27 dBm and -25 dBm channels produce essentially overlapping gain profiles and gain peaks at 1536 nm and 1544 nm wavelengths where some sharp jumps are visible. This is a result of parasitic lasing, which is more noticeable with lower input signal power. This unstable lasing effect can temporarily reach power levels over 10 dB above the amplified input signal. This spontaneous lasing becomes more prominent for longer spans of the erbium (Er^{3+})/ytterbium (Yb^{3+})-co-doped fiber in terms of changes in peak power and wavelength. Since the data presented is the average gain of each channel, in Fig. 6 the parasitic lasing effect is not as visible as it would be in an optical spectrum analyzer (OSA). However, it appears as distinct spikes when compared to adjacent channels.

When the pump source power is further increased to 2.0 W, for shorter erbium (Er^{3+})/ytterbium (Yb^{3+})-co-doped fiber span lengths of 2 m and 3 m, the overall channel gain continues to increase, with little emphasis on the gain peaks. However, with 5 m and 7 m erbium (Er^{3+})/ytterbium (Yb^{3+})-co-doped fiber span lengths, gain enhancement becomes apparent with input carrier signal powers between -27 dBm and -20 dBm in the channel, where the channel gain is nearly identical across the optical spectrum. The unevenness of the gain curve (jumps in the optical spectrum) is probably caused by the increased parasitic lasing effect, seen in Fig. 6 (c). Furthermore, setting the channel power even lower results in more intense parasitic lasing even for shorter fiber spans. The exact factors responsible for the initiation of lasing are not clear, but since longer spans of 5 meters increase the unwanted lasing, it appears to be related

to the inner cladding geometry of the fiber, which directs the multimode pumping laser to the doped core.

After propagation into the amplifier, most of the total gain is achieved in the first meters of the erbium (Er^{3+})/ytterbium (Yb^{3+}) -co-doped fiber. The input power in the channel and the pump power's total signal power at the amplifier's output remain effective within the span length of 2 m to 7 m erbium (Er^{3+})/ytterbium (Yb^{3+}) -co-doped fiber. Increasing the length of the erbium (Er^{3+})/ytterbium (Yb^{3+}) -co-doped fiber uses more pump light to maintain the achieved power level and redistribute the power to longer wavelengths, while lower wavelengths are gradually absorbed as the pump power decreases and cannot provide enough energy to maintain the power already achieved level. The combination of low input signal power and high pump power can lead to very noticeable gain locking due to the parasitic lasing effect, which becomes more intense in proportion to the length of the doped fiber. The same laser can reduce the power level achievable by nearby channels. This can be avoided by ensuring the input signal is strong enough to exceed the laser threshold.

In **Section 3.6**, the hybrid Raman-EDFA amplifier is created and performance analysis in the WDM transmission system is performed. Two main solutions for optical amplifiers are considered: erbium-doped fiber amplifiers (EDFA) and Raman fiber amplifiers. Raman amplifiers based on dispersion compensation fiber (DCF) have potential application in future optical communication systems, since CD compensation of chromatic dispersion in the fiber transmission line part can be obtained simultaneously with the amplification of the beneficial optical signals. In order to achieve the optimum operation of the amplifier, it is possible to create a hybrid Raman and erbium fiber optical amplifier (Raman-EDFA) solution to improve the optical signal-to-noise ratio (OSNR) performance in optical transmission systems. Therefore, to ensure the optimal solution for the enhanced creation of the hybrid Raman-EDFA, the experimental mathematical modeling was performed in the RSoft OptSim software environment. A variant of the experimental scheme was used with an erbium amplifier at the beginning of the EDFA and a Raman amplifier at the end of the line. The schematic in Fig. 7 represents the system in the RSoft OptSim software environment.

As we can see in Fig. 7, the WDM transmission system is divided into three parts: central office (CO), optical distribution network (ODN), and optical network terminal (ONT).

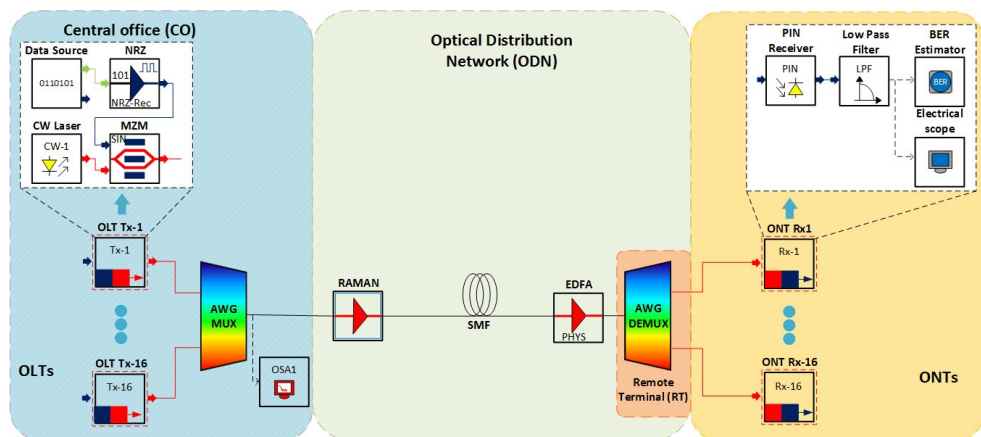


Fig.7. A scheme of 16-channel with 100 GHz spaced WDM transmission system with Raman-EDFA amplifier.

Each of the 10 Gbit/s transceivers Tx for optical line terminal (OLT), e.g. (OLT-Tx), consists of a data source, an NRZ-OOK encoder, a continuous wavelength (CW) laser and a Mach-Zehnder modulator (MZM). The CO consists of an optical line terminal (OLT) with sixteen transmitters (OLT_Tx), sixteen continuous wavelength (CW) lasers, an optical 16 x 1 power combiner where the signal is transmitted to an AWG multiplexer and an AWG demultiplexer with an insertion loss of 6 dB. Experimentally, the optimal power for continuous wavelength (CW) lasers was determined to be 4 dBm. Central frequencies for continuous wavelength (CW) lasers were set between 193.3 THz and 198.4 THz with 100 GHz inter-channel spacing. The optical distribution network (ODN) consists of a Raman amplifier, 6 km long dispersion compensating fiber (DCF) with an insertion loss of 0.55 dB/km.

The Raman amplifier uses a pumping power of 500 mW (26.98 dBm) and a pumping wavelength of 1455.30 nm, i.e. 206 THz. A single-mode optical fiber (SMF) according to the ITU-T G.652 recommendation in ODN segment is ≥ 40 km long, according to the ITU-T G.989.2 recommendation [160] with an attenuation factor of 0.2 dB/km and a dispersion of 16 ps/nm/km at 1550 nm. The EDFA amplifier uses a pumping source with a wavelength of 980 nm, i.e. 305.91 THz. The length of the erbium-doped fiber is up to 6 m. Each ONT receiver Rx, e.g. (ONT Rx), consists of an optical receiver based on a photodiode PIN with a sensitivity level of -20 dBm at a bit rate of 10 Gbit/s. The received modulated signal is then filtered with a low-pass electric filter LPF (3-dB bandwidth is 7.5 GHz). The quality of the received signal is evaluated, as measured by the BER Counter. According to the IEEE P802.3CS standard, the BER threshold corresponds to 1×10^{-9} .

The objective is to evaluate the performance of the hybrid Raman-EDFA amplifier in terms of global gain (GN), noise figure (NF) and BER. Two different pump laser cases were analyzed considering a hybrid amplifier configuration with two stages (Raman and EDFA). This hybrid amplifier configuration consists of two stages: a Raman amplifier and an EDFA amplifier. A Raman amplifier uses forward pumping, “co-propagating”, while an EDFA amplifier uses pumping in the opposite direction “counter-propagating”.

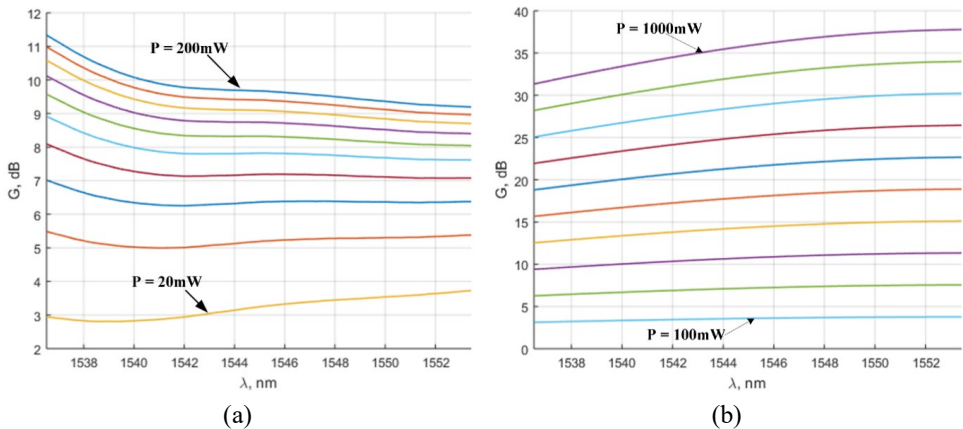


Fig. 8. Measured global gain: (a) of EDFA amplifier while choosing the pump power from 20 mW up to 200 mW with a 20 mW step; (b) noise figure of RAMAN amplifier while choosing the pump power from 100 mW up to 1000 mW with a 100 mW step.

To analyse optical gain of the Raman amplifier several experiments were performed. As it can be seen in Fig. 2 (a), the results reflect stability within the whole range of wavelengths with some deviations. Various power was used to analyze the stability of gain. The power of the Raman amplifier varied from 100 mW (the bottom curve) to 1000 mW (the top curve). It is possible to observe that at low powers, the optical gain only slightly depends on the signal wavelength. However, when increasing the power of Raman amplifier, it is possible to see that larger wavelength produces larger gain and also at higher powers dependency of the gain on the wavelength is more obvious.

As it shown in Fig. 8 (b), the EDFA amplifier gain was obtained by performing several experiments with variable wavelength and at different powers (the bottom curve corresponds to EDFA power of 20 mW, the top curve – 200 mW). It was observed that optical gain has similar behaviour at various powers, and the larger is the output of EDFA amplifier, the higher is the gain. It is also observed that signal wavelength has some effect on the gain. In the range of the wavelength from 1536 nm up to 1542 nm, the drop of gain is observed, whereas in the range from 1542 nm up to 1554 nm, the behaviour of the gain graph is more stable, and in some cases, the gain increases together with the wavelength, especially when the power of EDFA amplifier is lower than 40 mW (see the last two curves in the graph).

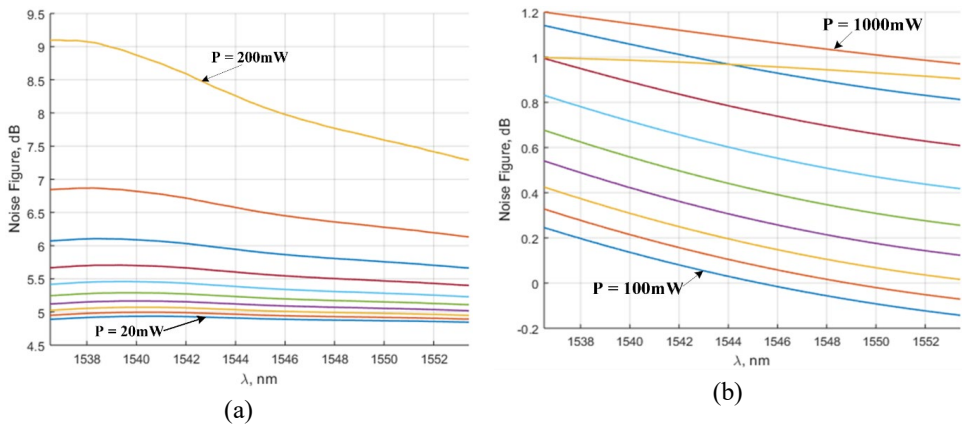


Fig. 9. Measured noise figure (a) of EDFA amplifier while choosing the pump power from 20 mW up to 200 mW with a 20 mW step, (b) global gain of RAMAN amplifier while choosing the pump power from 100 mW up to 1000 mW with a 100 mW step.

As it can be seen in Fig. 9 (a), the noise figure of the EDFA amplifier generally shows that at low powers, that is, below 140 mW, it slightly depends on the wavelength. At higher power values, for instance, 200 mW or 180 mW, the noise figure shows a remarkable dropdown when increasing the wavelength. After a series of experiments was performed, it was obtained that it is possible to obtain a low noise figure, i.e. the value is below 5 dB, using EDFA amplifier with power less than 60 mW. Moreover, at low powers the noise figure only slightly depends on the wavelength. Whereas at high powers significant drop can be observed when using different wavelengths.

As shown in Fig. 9 (b), the noise figure of the Raman amplifier describes experiments performed at different power values (from 100 mW for the bottom curve up to 1000 mW for

the top curve). It is observed that the noise level slightly depends on the wavelength – an increase in the signal wavelength decreases the noise level. In some cases, the noise level drops to negative values, especially when the power of the Raman amplifier is low (less than 200 mW). Interesting behaviour is observed at the power of Raman amplifier equal to 800 mW. In this case the drop in noise is minimal (less than 20 %). In all other cases, a greater drop in noise is observed.

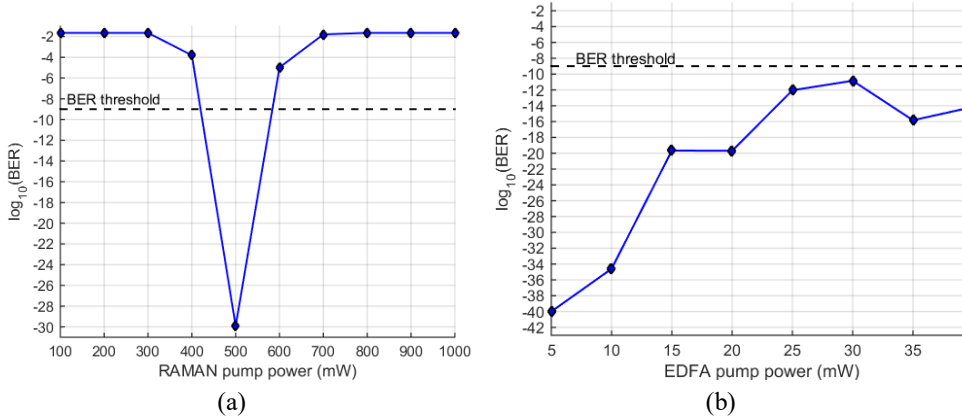


Fig. 10. a) *BER* versus (a) pump power of the Raman amplifier measured for the worst performing 8th channel of the proposed WDM system, while choosing the pump power from 100 mW up to 1000 mW with a 100 mW step; b) *BER* versus pump power of the EDFA measured for worst performing 8th channel of the proposed WDM system, while choosing the pump power from 5 mW up to 40 mW with a 5 mW step.

According to the simulation results, it can be considered that the maximal transmission distance, RAMAN amplifier pump power (at 100 mW to 600 mW), and EDFA amplifier (at 5 m to 40 m) at the *BER* threshold of 1×10^{-9} are the main criteria for the system's evaluation. The *BER* threshold of 1×10^{-9} has been reached after transmission over 500 mW of Raman span, and the system is operable at any EDFA power pump between 5 mW and 40 mW as the *BER* curves are below the 1×10^{-9} threshold over this range.

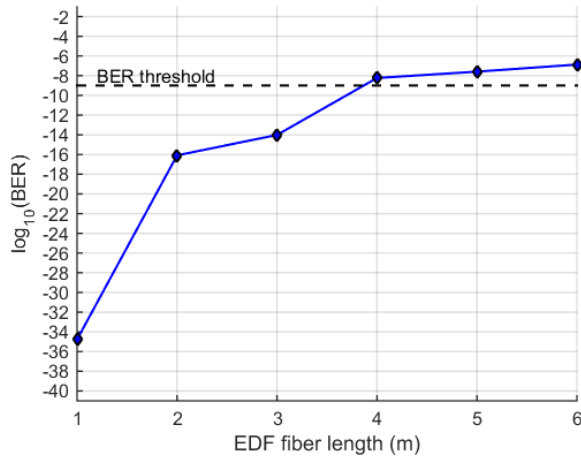


Fig. 11. *BER* depending on the fiber length.

Models of optical amplifiers and hybrid optical amplifiers were developed. The performance optimization of the hybrid EDFA-Raman amplifier was significantly improved due to the uniform gain bandwidth as well as the higher gain of the transmission system. The design of optimal hybrid amplifiers was critical to obtain broad gain and better noise performance. The parameters that optimized the EDFA performance in terms of noise figure and gain are EDF fiber length, input signal power, pump power, and pump wavelength, while the parameters that optimized the Raman amplifier are SMF fiber length and pump power. In the case of the Raman amplifier, the WDM transmission system operates with a pump power of 500 mW, and the pump source power of the EDFA amplifier was used in the range from 5 mW to 40 mW. A *BER* threshold of 1×10^{-9} is achieved after transmission over 3.8 m EDF span and ≥ 60 km SMF span.

MAIN RESULTS OF THE DOCTORAL THESIS

1. By performing the evaluation application of EDFA and SOA amplifiers to achieve the maximum transmission distance in DWDM system solutions, a mathematical calculation model was created in Matlab software, which was adjusted with the Rsoft Optsim simulation environment. Accordingly, a transmission system was developed, which consists of a CW laser source split into four constant optical carriers with a power level of 0 dBm, each driven by 25 Gbit/s pseudo-random bit sequence PRBS generators using electrical pulse generators and amplitude modulators, where 90° phase modulation was performed on two modulated optical carriers, which after phase modulation combined two signals with orthogonal phases for further modulation. All four optical signals were combined and transmitted through a Gaussian filter, i.e. a 3-dB bandwidth equal to 35 GHz (both in the transmitter and receiver parts). The generated and combined optical signals are amplified with an EDFA amplifier model with a fixed optical output power of 14 dBm and $NF = 4.5$, or with an SOA amplifier model with 8 dBm signal gain, $NF = 8$ and 14 dBm typical saturation power (P_{sat}). The amplified optical signal was transmitted through SMF fiber according to ITU-T G.652 recommendation (using 40 km span for SOA systems and 80 km span for EDFA systems), with the introduced attenuation $\alpha = 0.2$ dB/km, effective area = $80 \mu\text{m}^2$, dispersion coefficient $D = 16$ ps/nm/km at a wavelength of 1550 nm, and Kerr's nonlinear coefficient $\gamma = 1.26$ 1/W/km.

The electronic dispersion compensation (EDC) module on the receiver side fully compensated the accumulated CD in the fiber segment part. The transmission length was emulated using an iteration loop function and specifying multiple fiber spans for the EDFA and SOA amplification systems. Five transmission lengths of 80 km, 160 km, 240 km, 320 km, and 640 km were used to meet the Q factor requirement of > 16 dB using a standard inter-channel spacing of $\Delta f = 50$ GHz.

After transmission, the 100 Gbit/s DP-QPSK signal was split into four 25 Gbit/s signals by a 4×4 QPSK splitter based on phase and polarization and then converted to electrical signals by a PIN photodiode, passed through an LPF filter in EDC, and detected by Q factor estimator (performed *BER* analysis).

The bandwidths of the amplifiers used were determined separately for the EDFA, which was standard C-band (1530–1565 nm) with 86 channels, and 1530–1605 nm for the SOA amplification systems, which have a total of 182 transmission channels amplified by the SOA. This distribution provided ≈ 2.12 times higher transmission power (18.2 TBit/s) and 7 % higher spectral efficiency than EDFA ($SE = 2.10$ and 1.96 bit/Hz), respectively.

The study evaluated and compared the power efficiency levels in the proposed replacement scenario when EDFA reinforced optical connection, where 86 channels of C-band are used. **The total capacity was doubled by using SOA instead, providing 182 transmission channels due to the wider gain bandwidth.** The power consumption levels were defined based on the available technical data sheets of the components: $P_{tx} = 19$ W for DP-QPSK transceivers; SOA $P_{soa_amp} = 4$ W; and EDFA power consumption $P_{edfa_amp} = 30$ W. The energy efficiency levels show that the system with SOA gain for one-bit transmission required less energy. This difference became more significant for longer transmission distances – from 1.6 % to 12.6 %, 80 km and 640 km past the OF lines, respectively. This proves that SOA and the relatively low cost of components could provide additional environmental and financial benefits. It was shown that taking into account the correlation between the nonlinear distortion

and the ratio between the input power $P_{in}(t)$ and the saturation power P_{sat} of the semiconductor amplifier, it was possible to adjust the transmission parameters so that the Q factor is greater than 16 dB in a 640 km long optical fiber line.

2. A solution for an innovative optical amplifier based on an erbium (Er³⁺)/ytterbium (Yb³⁺) -co-doped fiber was investigated, i.e. the gain changes were compared of optical carriers (operation wavelength (C-band) depending on the length of the -co-doped fiber span (length 2–7 m), where the output power of the used multimode pumping source is used in the range of 0.6 – 2.0 W. The core of the erbium (Er³⁺)/ytterbium (Yb³⁺) -co-doped fiber used in the development of the innovative amplifier solution is doped with erbium (Er³⁺) and ytterbium (Yb³⁺). It was determined as an atomic percentage of 0.06 % and 1.21 %, respectively. A high-power pumping source (multimode pumping source) with a central wavelength of 975 nm and a bandwidth of 6 nm, maintained at 30 °C with a thermoelectric cooler, was used to prevent fluctuations in its output wavelength and power. The input signal is generated by filtering the light produced by a superluminescent light-emitting diode (S-LED) with –10 dB peak optical output power and an optical signal bandwidth between 1526 nm and 1630 nm wavelength range. A wavelength selective switch (WSS) filters the S-LED and produces a spectrum limited to C-band, which, in turn, consists of 48 channels with 100 GHz inter-channel spacing and 37.5 GHz bandwidth for the settings-enabled WSS. This optical carrier signal contains

48-channel interpretation emulating optical carriers (modulated signal data channels in WDM transmission systems solution). In the experimental demonstration, a double-clad splitter/combiner on the output side of the erbium (Er³⁺)/ytterbium (Yb³⁺) -co-doped fiber is used to separate the pump light from the amplified signal.

The pump source, with the lowest output power level of 0.6 W, produces significant peak gain at 1536 nm wavelength, achieving 34 dB gain using a 2 m erbium (Er³⁺)/ytterbium (Yb³⁺) -co-doped fiber span with an optical carrier input power of –27 dBm. When the span of the erbium (Er³⁺)/ytterbium (Yb³⁺) -co-doped fiber is increased, this peak decreases, and the second peak at 1544 nm becomes more prominent, and the gain for longer wavelengths increases. For a 7 m long erbium (Er³⁺)/ytterbium (Yb³⁺) -co-doped fiber, a third peak appears at 1563 nm, but the peak at 1544 nm is reduced. This results in a relatively linear gain between the two wavelengths mentioned above.

The pump power in the range from 0.6 W to 1.0 W increases the gain for all channels, but the peak gain becomes even more noticeable. However, at a span length of 5 m erbium (Er³⁺)/ytterbium (Yb³⁺) -co-doped fiber, the input carrier optical signal in the –27 dBm and –25 dBm channels power levels produces essentially overlapping gain profiles and gain peaks at 1536 nm and 1544 nm wavelengths, where some sharp jumps are visible.

As the pump source power is increased to 2.0 W, for shorter erbium (Er³⁺)/ytterbium (Yb³⁺) -co-doped fiber span lengths between 2 m and 3 m, the overall channel gain continues to increase, with a slight emphasis on the gain peaks. However, with 5 m and 7 m erbium (Er³⁺)/ytterbium (Yb³⁺) -co-doped fiber span lengths, the gain enhancement becomes apparent with input carrier signal powers between –27 dBm and –20 dBm in a channel where the channel gain is linear across the optical spectrum.

Most of the total gain in the optical carriers is achieved in the first meters of the erbium (Er³⁺)/ytterbium (Yb³⁺) -co-doped fiber after propagation. The input power in the channel

and the pump power's total signal power at the amplifier's output remain effective within the span length of 2 m to 7 m erbium (Er^{3+})/ytterbium (Yb^{3+}) -co-doped fiber.

3. CD compensation using one dispersion compensation module DCM is sufficient for fiber optical WDM transmission systems operating up to 10 Gbit/s data transmission rate in the channel. The problem with a DWDM system is that the CD value for each channel varies depending on the center wavelength; therefore, it is impossible to compensate the CD uniformly for the whole WDM system. To solve this problem, an additional compensation stage is introduced in the experimental part – CD_{SL} compensation of chromatic dispersion slope. As part of solving this problem, the two most common line codes of the on-off keying OOK signal are used – the non-return-to-zero (NRZ) line code and the return-to-zero (RZ) line code, where the NRZ coded signal occupies the entire bit interval for a 1-bit representation. In contrast, the RZ signal occupies only a fraction of the bit interval, which depends on the duty cycle. Hence, the bandwidth of the NRZ-encoded signal is approximately half that of the RZ-encoded signal.

WDM FOTS depends on CD_{SL} compensation using two different optical fibers: standard single-mode optical fiber (SMF) according to ITU-T G.652 recommendation and non-zero dispersion shifted fiber (NZDSF) according to ITU-T G.655 recommendation. Both of these fibers are widely used in WDM transmission system solutions; more specifically, the effect of CD_{SL} compensation is determined to understand how its compensation affects the performance of a 16-channel WDM transmission system with a data transmission rate of 40 Gbit/s per channel.

There are several methods of compensating for CD_{SL} . One method of CD_{SL} compensation is called hybrid fiber design (HFD), which means splitting the fiber into multiple spans where each span consists of two fibers. The second CD_{SL} compensation solution provides CD compensation for each WDM channel separately in the receiver part after channel demultiplexing. In this method, each channel after the WDM splitter can be treated as a separate transmission line, so only CD compensation is required. The third method is called mid-range spectral inversion (MSSI), and in this method, the pulse is inverted in the middle of the fiber span. The fourth and final method is also the most common method, where CD_{SL} compensation is achieved using a dispersion compensation module (DCM). The DCM module can also consist of a dispersion compensating fiber (DCF) or a fiber Bragg grating (FBG), e.g. FBG-DCM. The difference is in that in order to achieve CD_{SL} compensation, an additional DCM unit must be inserted into the FOTS. The transmission line usually consists of an optical fiber and two DCM units – one for CD compensation and the other for CD_{SL} compensation.

The experimental implementation consists of the 16-channel DWDM system model created in the RSoft OptSim simulation software with a data transmission rate of 40 Gbit/s per channel. It was found that the DCM's location changes individual channels' performance in the 16-channel WDM system operating with the data rate of 40 Gbit/s per channel.

The highest performance improvement in a 16-channel WDM system with a data transmission speed of 40 Gbit/s can be achieved when CD_{SL} compensation is applied together with CD compensation. It was concluded that using DCF for CD compensation and FBG for CD_{SL} compensation and deploying them for symmetrical compensation will provide a 16-channel WDM transmission system with a data transmission rate of 40 Gbit/s per channel highest performance, not exceeding the BER of the received signal $\geq 1 \times 10^{-9}$.

4. The development of a hybrid Raman-EDFA amplifier solution considers two main optical amplifier solutions: erbium-doped fiber amplifiers (EDFA), and Raman fiber amplifiers. Raman amplifiers based on dispersion-compensated fiber (DCF) have potential applications in future optical communication systems, since the CD compensation of chromatic dispersion in the fiber transmission line part can be obtained simultaneously with the favourable optical signal intercalation. The Raman-EDFA solution improves the optical signal-to-noise ratio (OSNR) and performance in optical transmission systems.

To evaluate and validate the Raman-EDFA solution, a 16-channel DWDM transmission system was built, which was divided into three parts: the central office (CO), the optical distribution network (ODN), and the optical network terminal (ONT), which operated in the range of 193.3 THz to 198.4 THz (from 1550.9 nm to 1538.9 nm wavelengths) with an inter-channel interval of 100 GHz. The optical distribution network (ODN) consists of a Raman amplifier, 6 km long dispersion compensating fiber (DCF) with an input loss of 0.55 dB/km.

The Raman amplifier part uses a pumping power of 500 mW (26.98 dBm) as well as a pumping wavelength of 1455.30 nm, i.e. 206 THz. A single-mode optical fiber (SMF), according to the ITU-T G.652 recommendation via optical distribution network segment, is ≥ 40 km long according to the ITU-T G.989.2 recommendation with an attenuation factor of 0.2 dB/km and a dispersion factor of 16 ps/nm/km . The amplifier part of the EDFA uses a pumping source with a wavelength of 980 nm, i.e. 305.91 THz. The length of the EDF fiber is up to 6 m. Each ONT receiver (Rx), or ONT Rx, consists of an optical receiver based on a PIN photodiode (PIN) with a sensitivity level of -20 dBm at a bit rate of 10 Gbit/s.

The noise figure of the EDFA amplifier section generally shows that at low powers, i.e. below 140 mW, it is slightly wavelength dependent. The noise figure shows a significant drop with increasing wavelength at higher power values, such as 200 mW or 180 mW. It was found that obtaining a low noise figure below 5 dB is possible using an EDFA amplifier with a power of less than 60 mW. On the other hand, a significant drop can be observed at high powers using different wavelengths. The noise figure of the Raman amplifier part is somewhat dependent on the wavelength – increasing the signal wavelength reduces the noise level. At a Raman amplifier power equal to 800 mW, the noise drop is minimal (less than 20 %).

Accordingly, the maximum transmission distance was determined as dependent on (a) the pump power of the Raman amplifier (100 mW to 600 mW) and (b) the length of the EDF-doped fiber for the EDFA amplifier (5 m to 40 m) at a BER threshold of 1×10^{-9} . A BER threshold of 1×10^{-9} is achieved after transmission beyond the 500 mW Raman range, and the system is operable with any EDFA power pumping from 5 mW to 40 mW, as the BER curves are below the 1×10^{-9} threshold in this range.

The DWDM transmission system, in the case of the hybrid Raman-EDFA amplifier, operates with a pump power of 500 mW, and the pump source power of the EDFA amplifier was used in the entire range from 5 mW to 40 mW. **The BER threshold of 1×10^{-9} is reached after transmission over 3.8 m EDF span and ≥ 60 km SMF span.**

BIBLIOGRAPHY

- [1] Ericsson, Ericsson Mobility Report – November 2020, Ericsson. (2020) 36.
- [2] C. Knittle, IEEE 50 Gb/s EPON (50G-EPON), Opt. InfoBase Conf. Pap. Part F174- (2020) 2020–2022. <https://doi.org/10.1364/OFC.2020.Th1B.2>.
- [3] E. Desurvire, Erbium-Doped Fiber Amplifiers: Principles and Applications, Wiley, New York, 1994.
- [4] Hecht, J. Understanding Fiber Optics. Fourth Edition. – NJ: Prentice Hall, 2002. – 780 p. ISBN: 978-0-1302-7828-9.
- [5] Фриман, Р. Мир связи. Волоконно-оптические системы связи. 4-ое, дополнительное издание. – Москва: Техносфера, 2007. – 512 с. ISBN: 978-5-94836-154-3.
- [6] Horak, R. Webster's New World Telecom Dictionary. – NY: John Wiley & Sons, 2007. – 568p. ISBN: 978-0-4717-7457-0.
- [7] Thyagarajan, K., Ghatak, A. *Fiber Optic Essentials*. NY: John Wiley & Sons, 2007. – pp. 86–259. ISBN: 978-0-470-09742-7.
- [8] Richardson, D. J., Fini, J. M., Nelson, L. E. Space-division multiplexing in optical fibres. *Nature Photonics*. Vol.7, 2013, pp. 354–362.
- [9] Chomycz, B. Planning Fiber Optics Networks. USA: McGraw Hill Professional, 2009, 320 p. ISBN: 978-0-07-164269-9.
- [10] Bobrovs, V., Ivanovs, G. Parameter Evaluation of Dense optical Network. *Electronics and Electrical Engineering*. Vol. 68, No. 4, 2006, pp. 33–54.
- [11] Основные принципы технологии DWDM. https://t8.ru/?page_id=10788
- [12] Agrawal, G. P. *Fiber-Optic Communications Systems*. Third Edition. NY: John Wiley & Sons, 2002. 561 p. ISBN: 0-471-22114-7.
- [13] Gumaste, A., Antony, T. *DWDM Network Designs and Engineering Solutions*. USA: Cisco Press, 2002. 368 p. ISBN: 978-1-58705-074-9.
- [14] Agrawal, G. P. *Fiber-optic communication systems*. New York: John Wiley & Sons, 1997. 555 p.
- [15] Azadeh, M. *Fiber Optic Engineering*. USA: Springer, 2009. p. 376.
- [16] Freeman, R. L. *Telecommunication System Engineering*. Geneva: Wiley-Interscience, 2004. p. 1024.
- [17] Agrawal, G. *Fiber-Optic Communication Systems*. USA: John Wiley and Sons, 2002. 561 p.
- [18] Bob Chomycz. *Planning Fiber Optic Networks*. USA: The McGraw-Hill Companies Inc., 2009, 401 p.
- [19] ITU-T G.957. Optical interfaces for equipments and systems relating to the synchronous digital hierarchy. International Telecommunication Union. 2006. pp. 1–38.
- [20] ITU-T G.984.2. Gigabit-capable Passive Optical Networks (G-PON): Physical Media Dependent (PMD) layer specification. International Telecommunication Union. 2003. pp. 1–28.
- [21] Thyagarajan, K. S., Ghatak, A. *Fiber Optic Essentials*. USA: Wiley–IEEE Press, 2007. p. 259.
- [22] ITU-T G.694.1. Spectral grids for WDM applications: DWDM frequency grid International Telecommunication Union. 2012. pp. 1–16.
- [23] ITU-T G.694.2. Spectral grids for WDM applications: CWDM wavelength grid. International Telecommunication Union. 2003. pp. 1–12.
- [24] Becker, P. C., Plsson, N. A., and Simpson, J. R. “Erbium Doped Fiber Amplifiers”, Academic Press, USA, 1999, 481 p.
- [25] Islam, M. N. “Raman amplifiers for telecommunications 2”, Springer, USA, 2004, pp. 298–463.
- [26] Dutta, A. K., Dutta, N. K., and Fujiwara, M. “WDM technologies active optical components”, Academic Press, 2002, 710 p.

- [27] Laming, R. I., Zervas, M. N., Payne, D. N. “Erbium Doped Fiber Amplifier with 54 dB Gain and 3.1 dB Noise Figure”, *IEEE Photonics Technology Letters*, Vol. 4, No. 12, 1992, pp. 1345–1347.
- [28] Лохманов, П. Мощный волоконно-оптический эрбиевый усилитель для для многоканальных DWDM систем. Магистерская диссертация. Москва: МГТУ МИРЭА, 2014. 48 с.
- [29] Лазеры накачки. <http://journals.ioffe.ru/articles/viewPDF/10386>
- [30] Kenneley, P. L., Kaminow, I. P., Agrawal, G. P. “Nonlinear Fiber Optics. Third Edition”, USA: Academic Press, 2001, p. 481.
- [31] Felinskyi, G. S., Korotkov, P. A. “Raman Threshold and Optical Gain Bandwidth in Silica Fibers”, *Quantum Electronics & Optoelectronics*, Vol. 11, No. 4, 2008, pp. 360–363.
- [32] Zhang, T., Zhang, X., Zhang, G. “Distributed fiber Raman amplifiers with incoherent pumping”, *Photonics Technology Letters, IEEE* , Vol. 17, No. 6, 2005, pp. 1175.–1177.
- [33] Connelly, M. J. “Semiconductor optical amplifiers”, University of Limerick, Ireland, 2004, 177 p. ISBN 978-0-306-48156-7
- [34] Rahman, T., Rafique, D., Napoli, A., de Man, E., Spinnler, B., Bohn, M., Okonkwo, C. M., Koonen, A. M. J., and de Waardt, H. “Ultralong Haul 1.28-Tb/s PM-16QAM WDM Transmission Employing Hybrid Amplification”, *Journal of Lightwave Technology*, Vol. 33, No. 9, pp. 1794.–1804, May 1, 2015.
- [35] Reichmann, K. C., Iannone, P. P., Zhou, X., Frigo, N. J., Hemenway, B. R. “240-km CWDM Transmission Using Cascaded SOA Raman Hybrid Amplifiers With 70-nm Bandwidth”, *IEEE Photonics Technology Letters*, Vol. 18, No. 2, 2006, pp. 328–330.
- [36] OFS Specialty Photonics Division. (2013). Highly Non-Linear Fiber (HNLF). Product Sheet, Version: 20131210, Denmark, 1, 2013.
- [37] Pavlovs, D., Bobrovs, V. Relationship between spectral efficiency and energy efficiency in 10 Gbps NRZ-OOK, 40 Gbps NRZ-DPSK and 100 Gbps DP-QPSK WDM transmission systems. In: *Progress in Electromagnetic Research Symposium (PIERS 2016)*, 8–11 August 2016, pp.1434–1438. Shanghai, China. doi:10.1109/PIERS.2016.7734673
- [38] Van Heddeghem, W., Idzikowski, F., Vereecken, W., Colle, D., Pickavet, M., De-meester, P. (2012). Power consumption modeling in optical multilayer networks. *Photonics Network Communications*, 24(2), 86–102. doi:10.1007/s11107-011-0370-7
- [39] Iyer, S., & Singh, S. P. (2016). Spectral and power efficiency investigation in single- and multi-line-rate optical wavelength division multiplexed (WDM) networks. *Photonics Network Communications*. doi:10.1007/s11107-016-0618-3
- [40] Agrawal, G. P. (2007). *Nonlinear Fibre Optics*. New York, NY, USA: Academic.
- [41] Velasco, L., Jirattigalachote, A., Ruiz, M., Monti, P., Wosinska, L., & Junyent, G. (2012). Statistical approach for fast impairment-aware provisioning in dynamic all-optical networks. *IEEE/OSA Journal of Optical Communications and Networking*, 4 (2), 130–141. DOI: 10.1364/JOCN.4.000130
- [42] Bendimerad, D. F., & Frignac, Y. (2017). Numerical Investigation of SOA Nonlinear Impairments for Coherent Transmission Systems Based on SOA Amplification. *Journal of Lightwave Technology*, 35 (24), 5286–5295. DOI: 10.1109/JLT.2017.2772223
- [43] Zakis, K., Olonkins, S., Udalcovs, A., et al. Cladding-Pumped Er/Yb-Co-Doped Fiber Amplifier for Multi-Channel Operation. *Photonics*, 2022, 9, 457.
- [44] Supe, A., Olonkins, S., Udalcovs, A., et al. Cladding-Pumped Erbium/Ytterbium Co-Doped Fiber Amplifier for C-Band Operation in Optical Networks. *Appl. Sci.*, 2021, 11: 1702.
- [45] ITU-T Recommendation G.989.2, “Digital sections and digital line system – Optical line systems for local and access networks-40-Gigabit-capable passive optical networks 2 (NG-PON2): Physical media dependent (PMD) layer specification”, 2012.



Mareks Parfjonovs was born in 1983, in Liepāja. He received a Master's degree of Social Science in Economics from Riga Technical University in 2010. He is currently a researcher at the Institute of Photonics, Electronics and Electronic Communications of RTU Faculty of Computer Science, Information Technology and Energy.